ELEMENTA
Science of the Anthropocene

RESEARCH ARTICLE

Increases in Arctic sea ice algal habitat, 1985—2018

Stephanie M. Lim[1],*, Courtney M. Payne[1], Gert L. van Dijken[1], and Kevin R. Arrigo[1]

In the Arctic Ocean, sea ice algae are responsible for a small but seasonally important pulse of primary production. Their persistence is threatened by the rapid loss of sea ice from the Arctic Ocean due to climate change, but this threat will be at least partially offset by the replacement of multiyear ice (MYI) with first-year ice (FYI). FYI is thinner and usually features a thinner snow cover than MYI, thus transmitting more light to support ice algal growth. We combined remote sensing, reanalysis data, and modeling products with a radiative transfer model to assess how the changing physical conditions in the Arctic altered the extent and duration of the bottom ice algal habitat over a 34-year period. Habitat was defined as areas where enough light penetrates to the bottom ice to support net positive photosynthesis. The Arctic shifted from 37% FYI in 1985 to 63% in 2018, as the 2.0×10^6 km^2 increase in FYI extent outpaced the 0.6×10^6 km^2 decrease in overall sea ice extent above the Arctic Circle. The proliferation of younger ice corresponded with a 0.08 m decade^{-1} decrease in average sea ice thickness and a 0.003 m decade^{-1} decrease in average snow depth. The end of the ice algal season, marked by the onset of warm summer air temperatures, moved slightly earlier, by 1.4 days decade^{-1}. Our analysis indicates that ice algal habitat extent increased by 0.4×10^6 km^2 decade^{-1}, or from 48% to 66% of total sea ice extent. The average ice algal growing season also lengthened by 2.4 days and shifted earlier in the year. Together, these trends suggest that net primary production in Arctic sea ice increased during 1985–2018. The most dramatic changes were localized in the Central Basin and the Chukchi Sea and were driven primarily by the declining snow cover and the shift from MYI to FYI. Although the Arctic recently became more favorable to ice algae, we expect that this trend will not continue indefinitely, as a limited amount of MYI remains.

1. Introduction

Sea ice algae are found in all regions of the Arctic Ocean, from the deep Central Basin to the surrounding shelf seas (Arrigo, 2017) and are responsible for a small but seasonally important pulse of primary production. They contribute an estimated 9–73 Tg C yr^{-1}, or about 2–10% of total Arctic primary production, but can account for up to 40% in locations with low phytoplankton production (Subba Rao and Platt, 1984; Legendre et al., 1992; Deal et al., 2011; Dupont, 2012; Jin et al., 2012; Watanabe et al., 2019). Critically, they usually bloom 1–3 months before phytoplankton (Ji et al., 2013; Payne et al., 2021), they serve as a rich food source for both sympagic (ice-associated) grazers (Nozais et al., 2001; McConnell et al., 2012; Bluhm et al., 2017; Caron et al., 2017) and early season zooplankton (Runge and Ingram, 1988; Søreide et al., 2010; Durbin and Casas, 2014), and their impact can be traced up the food web (Kohlbach et al., 2016). The remaining ice algal biomass can be exported to the

seafloor where it likely contributes to benthic food webs and remineralization processes (Ambrose et al., 2005; Renaud et al., 2007; Boetius et al., 2013; Wiedmann et al., 2020). The release of algae from melting sea ice may serve to seed phytoplankton blooms, though the magnitude and duration of that contribution may be variable or limited (Syvertsen, 1991; Tedesco et al., 2012; Szymanski and Gradinger, 2016; Selz et al., 2018).

Microalgal growth in sea ice is influenced by many factors, beginning with the incorporation of algae into the ice during its formation and growth (Garrison et al., 1983; Gradinger and Ikävalko, 1998; Różańska et al., 2008; Olsen et al., 2017; Kauko et al., 2018). Strong salinity and temperature gradients within the sea ice interior, which control the porosity and connectedness of the brine network, limit available space and generally make the bottom ice a more suitable habitat (Tedesco and Vichi, 2014; Leu et al., 2015). For ice algae to grow, enough light must be transmitted to the algal layer to support net photosynthesis; the transmission of this light depends on the incoming solar radiation, attenuation in the atmosphere, photoperiod as the Arctic transitions out of polar night, thickness of the snow and ice, and optical properties of snow (determined by grain size and wetness) and sea ice (determined

[1] Department of Earth System Science, Stanford University, Stanford, CA, USA

*Corresponding author:
Email: smlim@stanford.edu

by brine volume, bubble content, and soluble and particulate matter content). Light availability is usually the limiting factor in ice algal bloom initiation (Lavoie et al., 2005; Tedesco and Vichi, 2014; Mortenson et al., 2017) and, in particular, is strongly tied to the depth of the snow pack (Welch and Bergmann, 1989; Bergmann et al., 1991; Rysgaard et al., 2001; Leu et al., 2015), as the attenuation of light by snow is much greater than by sea ice (Perovich et al., 1986; Stroeve et al., 2021). Sea ice thickness is thought to be a secondary control on light transmission but can still be important, particularly on kilometer scales (Katlein et al., 2015). Nutrients, which are supplied by seawater exchange or are internally recycled (Meiners and Michel, 2017), also control where algae grow in the sea ice and often determine bloom magnitude (Lavoie et al., 2005; Tedesco and Vichi, 2014; Mortenson et al., 2017). Though grazers certainly consume ice algae, they are not usually considered controls on ice algal blooms (Werner, 1997; Nozais et al., 2001). Most blooms end when ice algae slough off the bottom of the sea ice as atmospheric conditions (air temperatures or rain) and the transmission of heat through the snow and ice cause the bottom of the ice to melt (Fortier et al., 2002; Lavoie et al., 2005; Selz et al., 2018; Oziel et al., 2019). Warmer seawater temperatures can also contribute to bottom ice melt (Perovich, 2011).

Of the many aspects of the Arctic that have responded rapidly to climate change, among the best documented and quantified are changes to the atmosphere and the physical marine environment. Both Arctic air and water temperatures have warmed at more than twice the global rate (Arctic Monitoring and Assessment Programme [AMAP], 2019; Carvalho and Wang, 2020). An increase in summer clouds has decreased photosynthetically active radiation (PAR, 400–700 nm) incident on the ocean surface (Bélanger et al., 2013). Sea ice has declined by every metric—areal extent, thickness, age, volume, seasonal duration—and the rate of decline has been increasing (Stroeve and Notz, 2018; AMAP, 2019). From 1979 to 2018, the Arctic lost 11% of its sea ice as measured during the maximum extent in March and 45% as measured during the minimum extent in September (Stroeve and Notz, 2018). Sea ice decline has not been equally distributed among regions, but has been concentrated in the lower-latitude peripheral seas (Onarheim et al., 2018). Most of the Arctic has also experienced a shorter sea ice season, which declined by 0.5–1.5 days yr^{-1} between 1979 and 2013 (Parkinson, 2014). As less sea ice has been retained during summer, ice has become younger and thinner on average. Multiyear ice (MYI) extent declined by >50% over 1999–2017, and first-year ice (FYI) now makes up more than two-thirds of the Arctic sea ice cover (Kwok, 2018). This change has corresponded with a widespread decrease in ice thickness, from an Arctic end-of-melt average of 3.0 m in 1958–1976 to 1.0 m in 2011–2018 (Kwok, 2018). Changes in sea ice extent and thickness can also be monitored in terms of ice volume, which decreased by 2,870 km^3 $decade^{-1}$ during 2003–2018 (Kwok, 2018). Lastly, the average snow depth on Arctic sea ice in spring decreased by about 0.1 m between 1951–1991

and 2009–2013: field data in the western Arctic showed a decline from a mean depth of 0.35 m to 0.22 m (Webster et al., 2014), while modeling showed a pan-Arctic decline from 0.41 m to 0.31 m (Blanchard-Wrigglesworth et al., 2015). Rather than changes in snowfall rates or snow redistribution, the shift towards FYI has likely driven this decline, as MYI can accumulate more snow over its longer life span (Blanchard-Wrigglesworth et al., 2015).

The combined effect of these changes on Arctic ice algae is not immediately obvious. Their persistence is threatened by the rapid loss of sea ice, but this threat may be offset by the replacement of MYI with FYI. That is, ice algal habitat may be decreasing because less sea ice is available for a shorter period of time or, alternatively, it may be increasing because thinner FYI and snow transmit more light for photosynthesis. For example, Stroeve et al. (2021) found that thinner snow led to increased under-ice light in the Arctic's marginal seas in April and in the entire Arctic Ocean in July between 2011 and 2018. An intercomparison of five numerical Arctic marine ecosystem models exhibited no consistent trends in ice algal production over 1980–2009 despite thinning ice and snow, but demonstrated the importance of the balance between a stable sea ice cover (marked by thicker ice) and sufficient light transmission: there were both positive and negative correlations between ice algal productivity and maximum ice thickness (Watanabe et al., 2019).

In this study, we examined Arctic ice algal response to the reduction in overall sea ice extent and the increase in FYI over the 1985–2018 period. We combined remote sensing, reanalysis data, and modeling products with a radiative transfer model to assess changes in the extent and duration of the ice algal habitat. Here, the term "habitat" describes a physical environment that supports net positive photosynthesis by ice algae, based on sea ice and snow characteristics and the corresponding light transmission to the ice algal layer. This study focuses on spring blooms of bottom ice algae, which account for a majority of ice algal biomass and production in the Arctic Ocean (Leu et al., 2015; Arrigo, 2017). We chose not to model an accumulating ice algal pool nor consider nutrient availability due to the relatively sparse distribution of surface nutrient samples, particularly in the Central Basin (Codispoti et al., 2013; Randelhoff et al., 2020; Wiedmann et al., 2020). In relying more heavily on Arctic sea ice observations, we avoid the uncertainty present in many numerical models of Arctic sea ice algae, which show little agreement, especially on decadal time scales (Watanabe et al., 2019). Instead, the assessment focuses on how changing physical conditions have altered the amount of algal habitat over 34 years and the implications for the future of the Arctic Ocean in the face of global climate change.

2. Methods
The bottom layer of Arctic sea ice was assessed for its potential as ice algal habitat between 1985 and 2018. Atmospheric reanalysis, snow evolution modeling, and sea ice satellite and reanalysis products were used to characterize the physical ice environment and calculate whether
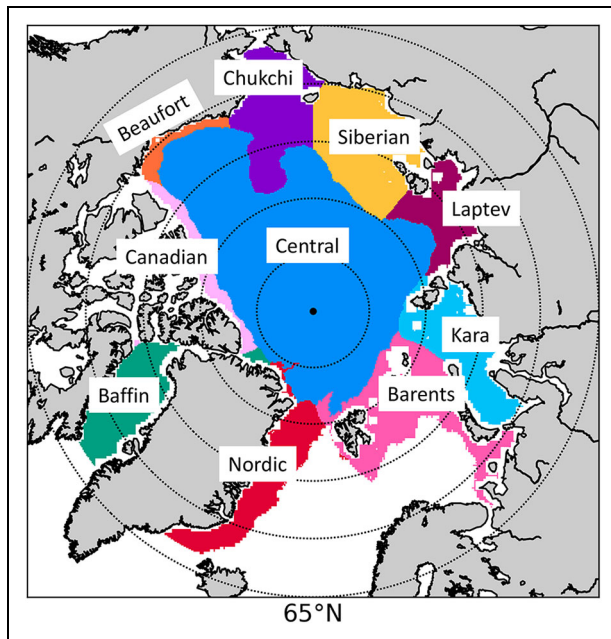
Figure 1. Arctic sea ice regions. Regions are superimposed on the winter ice extent in the year 2000. The Central Basin is defined by the 1,000 m isobath and is surrounded by the peripheral seas. The Barents and Chukchi seas are categorized as inflow shelves and Baffin Bay and the Canadian and Nordic regions are outflow shelves. The rest are interior shelves. Dotted black circles are lines of latitude, 5° apart.

the PAR transmitted to the bottom of the ice was sufficient to support net positive ice algal photosynthesis. All inputs were regridded in NASA SeaDAS (version 7.5.3) to a 12.5 km polar stereographic grid. Habitat potential was determined each day from January to July for all sea ice above the Arctic Circle at 66.5°N.

2.1. Arctic regions

Most sea ice in the Arctic is free-drifting and can move substantially over the course of the ice season. Our assessment did not explicitly account for ice floe movement and instead treated the Arctic as a Eulerian set of spatially fixed sea ice pixels. As a result, characterizing habitat suitability and duration at the 12.5 km pixel scale over 7 months would be somewhat inaccurate. Light transmission and ice algal photosynthesis were calculated every 3 h at the pixel scale to capture the daily spatial variability, but all annual characteristics (e.g., ice freeze-up, yearly average snow depth) and results are analyzed on larger spatial scales (regions, latitudinal bands, or pan-Arctic). We divided the Arctic Ocean into regions defined by their bathymetry and flow patterns (**Figure 1**; **Table 1**; Carmack et al., 2006; Lewis et al., 2020). The Central Basin, the deepest (about 4,000–4,500 m) and largest of the regions, is separated by the 1,000 m isobath from three types of peripheral seas (about 50–300 m): interior shelves (the Beaufort, Siberian, Laptev, and Kara seas), inflow shelves (the Chukchi and Barents seas), and outflow

shelves (Baffin Bay and the Canadian and Nordic regions). Given the size of these regions and the mostly zonal movement of sea ice in the Arctic (Wei et al., 2019), sea ice largely remains within the same region for a single January–July period, making a region a useful unit for yearly assessment and analysis. Note that the Canadian Arctic Archipelago was omitted from most of our analyses due to insufficient sea ice data.

2.2. Ice algal habitat potential

The Arctic EASE-Grid sea ice age product (Version 4, 12.5 km, weekly resolution; Tschudi et al., 2019) was used to approximate sea ice thickness (**Figure 2B** and **C**) from 1985 to 2018. The ice age product uses Lagrangian tracking to track the motion and age of each ice parcel. Although some remotely sensed ice thickness products exist, they do not span the length of this time series, while using the multi-decadal record of ice age enables longer and more consistent coverage (Tschudi et al., 2020). We leveraged the fact that ice age is strongly related to ice thickness (Maslanik et al., 2007; Tschudi et al., 2016) to obtain spatial information on sea ice thickness.

First, ice age, given in years, was converted to ice age in days, based on the number of days since freeze-up. The freeze-up date for each year was approximated as the date when a specified proportion (0.5 in the standard run; **Table 2**) of a 2° latitudinal band in a "grouped region" was ice-covered. The grouped regions were 1) the Central Basin, 2) the Chukchi and Beaufort seas, 3) the Canadian Arctic, Baffin Bay, and Nordic region, 4) the Barents Sea, and 5) the Kara, Laptev, and Siberian seas. Because ice may freeze as early as September and the ice algal assessment is run through the following July, ice age is the parameter most likely to be affected by sea ice motion. Having grouped regions that were wide in the east-west direction, but narrow in the north-south direction was a compromise between retaining ice within the same grouped region all year and characterizing freeze-up on a finer spatial scale.

The following saturating function was then used to determine ice *thickness* (m) from *age* (d):

$$thickness = max \frac{age}{k + age} \qquad (1)$$

where an ordinary least squares regression calibrated with the Tschudi et al. (2016) compilation of average spring (February–March 2004–2008) Ice, Cloud, and land Elevation Satellite (ICESat) ice thicknesses gave $k = 155.08$ d^{-1} and $max = 2.90$ m. Ice >5 years old was omitted from the regression because higher age estimates are considered imprecise (Tschudi et al., 2019), but was included in the actual assessment.

Snow depth inputs were from SnowModel-LG, a Lagrangian snow evolution model (Version 1, daily, 25 km resolution; Liston et al., 2020; Stroeve et al., 2020). We used the SnowModel-LG product forced by the European Centre for Medium-Range Weather Forecasts ReAnalysis-5th Generation (ERA5; **Figure 2D**). Because snow depth is expected to vary substantially within each pixel (Mundy et al., 2005; Abraham et al.,

Table 1. Yearly maximum ice extent mean and standard deviation (SD) for each region, 1985–2018 (n = 34)

Region	Maximum Ice Extent	
	Mean (km^2)	SD (km^2)
Central	4,062,647	495
Chukchi	697,495	0[a]
Beaufort	117,546	0[a]
Baffin	541,020	392
Nordic	647,785	127,052
Barents	868,024	144,243
Kara	606,452	2,106
Laptev	378,894	0[a]
Siberian	895,675	218
Pan-Arctic	9,049,555	244,731

[a] For some regions, the ice extent does not vary, as the winter ice extent above the Arctic Circle is not changing, unlike ice extent in other seasons or areas of the Northern Hemisphere.

2015), we applied a subpixel snow depth distribution to each pixel. Although ice thickness will also vary on the subpixel spatial scale, snow depth variability is expected to have a greater effect on light transmission and thus ice algal habitat, in part because snow has a much higher diffuse attenuation coefficient (K_d) than ice (Perovich et al., 1986). Furthermore, the range of snow depths within one pixel is greater than that of ice and can span one to two orders of magnitude (Mundy et al., 2005). Each pixel was divided into nine subpixels. The SnowModel-LG snow depth was treated as the average for the pixel, and for each subpixel was multiplied by one of nine multipliers (0.102, 0.272, 0.427, 0.532, 0.721, 0.952, 1.310, 1.740, 3.310). The multipliers approximate a lognormal distribution (mean = 1, standard deviation = 0.25) that matches the in situ snow distribution on Antarctic sea ice (Arrigo et al., 1998) but should also apply here.

The PAR penetrating the ice and snow in each subpixel was determined following Arrigo et al. (1991). Diffuse and direct downwelling surface irradiance at the air-snow or air-ice interface were calculated using a spectral atmospheric radiative transfer model (**Figure 2A**; Gregg and Carder, 1990; Arrigo et al., 1998). Atmospheric inputs were from the National Centers for Environmental Prediction/National Center for Atmospheric Research (NCEP/NCAR) Reanalysis Project 1 (4x daily, T62 Gaussian grid; Kalnay et al., 1996) and NASA's Ozone Record (daily, 1° resolution). Surface irradiance was also corrected for clouds (Dobson and Smith, 1988). The surface specular reflection of incident irradiance was based on the surface type: specular reflection was 5% of diffuse and direct light for snow and 5% of diffuse light and a sun angle-dependent percent of direct light for bare ice (Arrigo et al., 1991). The remaining

light was transmitted through the snow (if present) and ice layers, following Beer's law:

$$E_d(z, \lambda) = E_d(0, \lambda)e^{-K_d(\lambda)z} \qquad (2)$$

where $E_d(z,\lambda)$ is the spectral downwelling irradiance (μmol photons m^{-2} s^{-1} nm^{-1}) of wavelength λ (nm) at the bottom of a snow or ice layer of thickness z (m), $E_d(0,\lambda)$ is the spectral downwelling irradiance at the top of the layer, and $K_d(\lambda)$ is the spectral diffuse attenuation coefficient (m^{-1}) for that layer. Different K_d spectra were used for dry snow, a scattering layer of white ice, and interior white ice (**Table 2**; Perovich et al., 1986). $E_d(\lambda)$ was calculated at the top of the ice algal layer (**Table 2**) every 3 h and spectrally integrated to calculate the total PAR available to ice algae for each subpixel.

The gross chlorophyll a (Chl a)-specific photosynthetic rate (P, in g C g^{-1} Chl a h^{-1}) supported by the transmitted PAR (μmol photons m^{-2} s^{-1}) in each subpixel was calculated as:

$$P = P_{max}\left(1 - e^{-\frac{\alpha(PAR)}{P_{max}}}\right) \qquad (3)$$

where P_{max} is the maximum photosynthetic rate (g C g^{-1} Chl a h^{-1}) and α is the slope describing the relationship between irradiance and photosynthetic rate before light-saturation (g C g^{-1} Chl a h^{-1} [μmol photons m^{-2} s^{-1}]$^{-1}$). The values of P_{max} and α in the standard run were from a pan-Arctic compilation of photosynthetic parameters measured on bottom ice algae (**Table 2**; van Leeuwe et al., 2018). We averaged the values from pack and landfast ice cores. A similar compilation of Arctic P_{max} and α measurements was checked for a correlation to ice thickness or snow depth, but no consistent relationship was found—hence the choice to use constant values.

A constant Chl a-specific respiration rate (R, in g C g^{-1} Chl a h^{-1}), independent of transmitted PAR, was subtracted from P to calculate the net Chl a-specific photosynthetic rate. In the standard run, R was based on the dark respiration rate of ice algae in the bottom of FYI in Resolute Passage (**Table 2**; Suzuki et al., 1997). Light transmission and the corresponding net Chl a-specific photosynthetic rate were calculated every 3 h and integrated over 1 day for each subpixel. If the net Chl a-specific photosynthetic rate was >0 for the day, then the subpixel was considered potential habitat for ice algae. The subpixels were then spatially recombined to determine the proportion of each pixel that is potential habitat (range 0/9 to 9/9) each day (**Figure 2F**).

For a given year, the season of ice algal growth ended at each pixel when 2-m air temperatures (NCEP/NCAR Reanalysis 1) remained above 0°C for 96 h (**Figure 2E**). This metric approximates the time of year when both the snow and bottom ice begin to melt, causing algae to slough off the bottom of the ice (Lavoie et al., 2005; Oziel et al., 2019; Sorrell et al., 2021). The 96-h threshold distinguishes between a temporary warm period and the actual seasonal melt. If a pixel did not reach the 96-h threshold during January to July for a given year, then the melt date was set to July 31. Dates are often reported as the day of the year (DOY), ranging from 1 to 365.
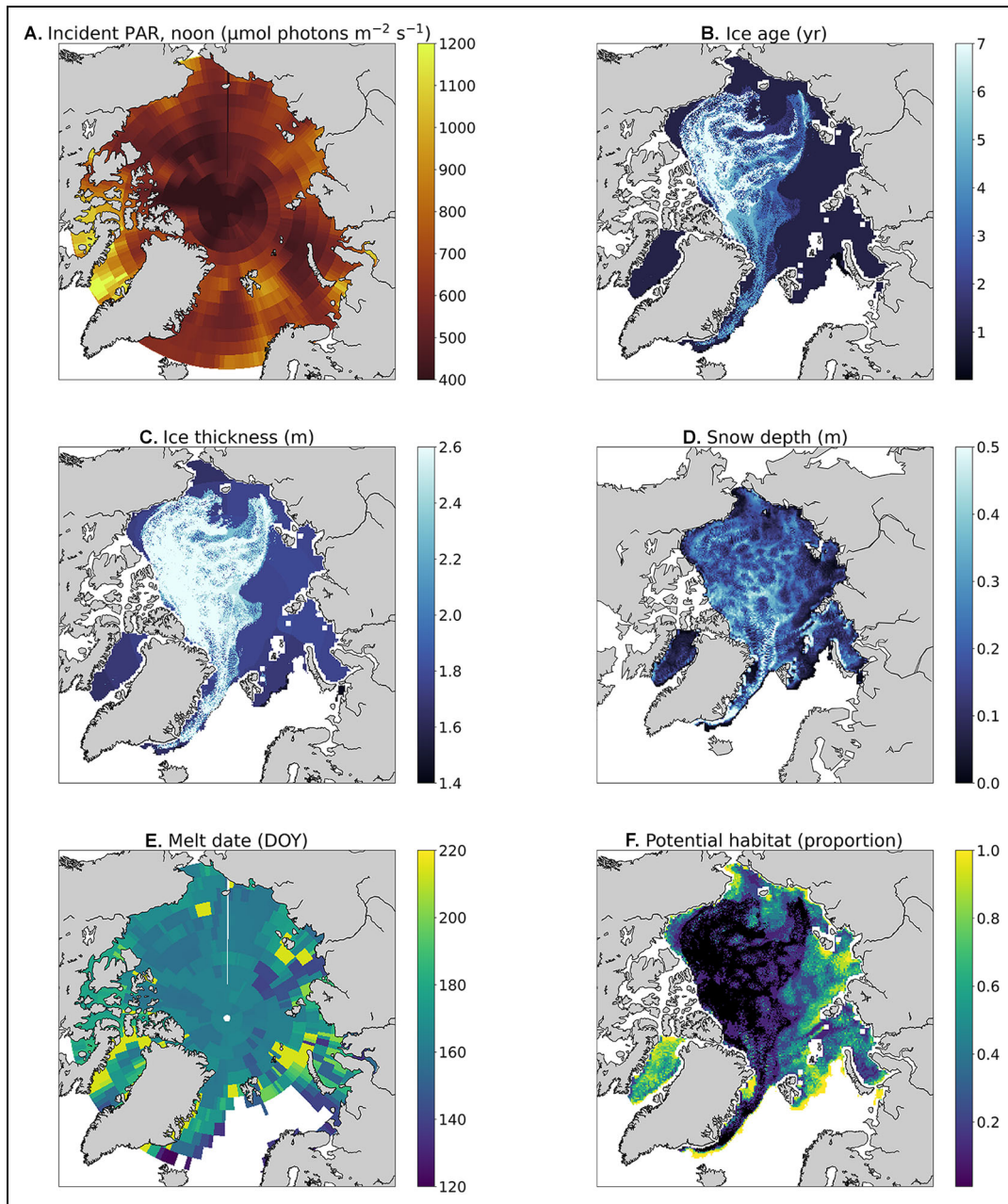
Figure 2. Examples of ice algal habitat assessment inputs and output. (A) Downwelling incident photosynthetically active radiation (PAR) at noon, (B) sea ice age, (C) sea ice thickness, (D) snow depth, (E) melt date reported as the day of the year (DOY), and (F) potential ice algal habitat. All plots show data for May 15, 2000, except for melt date, which is relevant for the entire year 2000.

2.3. Analysis and statistics

A metric of habitat-days (km^2 d) was developed to characterize the duration and location of potential ice algal habitat in the spring. The proportion of potential habitat was calculated for each day and summed from January to July for each pixel. All pixels were then summed spatially over different areas of interest for analysis: the entire Arctic, individual regions (**Figure 1**), and 5° latitudinal bands. Here we largely report normalized habitat-days (d), which normalizes the habitat-day metric by the maximum ice extent of the relevant area and can be thought of as the spatially averaged duration of potential habitat. That is, normalized habitat-days would equal the length of the ice algal growing season if 100% of the area was potential habitat or twice the length of the growing season if only 50% of the area was potential habitat.

Habitat-days is analogous to the unit of degree-days used in studies of the effects of ocean and atmospheric warming and incorporates several nuances that are particularly useful when examining Arctic ice algal habitat. Habitat-days accounts for variable snow depths, and thus variable habitat, on a subpixel scale. It also remains a useful large-scale metric despite moving ice floes and despite the extreme horizontal patchiness of ice algal habitat, because a large number of habitat-days could result from a few days of habitat over a large area or many days of

Table 2. Ice algal habitat assessment parameters

Parameter[a]	Standard Run Value	Units
P_{max}	0.70[b]	g C g^{-1} Chl a h^{-1}
α	0.10[b]	g C g^{-1} Chl a h^{-1} [μmol photons m^{-2} s^{-1}]$^{-1}$
Respiration rate	0.22[c]	g C g^{-1} Chl a h^{-1}
Scattering layer thickness	0.30[d]	m
Diffuse attenuation coefficient of dry snow	22.33[e]	m^{-1}
Diffuse attenuation coefficient of scattering ice	5.35[e]	m^{-1}
Diffuse attenuation coefficient of interior ice	1.68[e]	m^{-1}
Melt date threshold	96	h
Freeze-up threshold	0.5	unitless
Suitable habitat threshold	7.32	days
Algal layer location	0.05[f]	m

[a] P_{max} = maximum photosynthetic rate; α = the slope describing the relationship between irradiance and photosynthetic rate before light-saturation.

[b] van Leeuwe et al. (2018).

[c] Suzuki et al. (1997).

[d] Perovich (2002).

[e] Diffuse attenuation coefficients are spectral; here we report the mean for 400–700 nm (Perovich et al., 1986).

[f] Measured from the ice-water interface at the bottom of the sea ice (van Leeuwe et al., 2018).

habitat over a small area. For example, both 1 km^2 of sea ice that is potential habitat for 10 days and 5 km^2 of sea ice that is potential habitat for 2 days would be measured as 10 habitat-days. Furthermore, the habitat-days calculation does not assume that ice algal habitat is continuous over the course of a year, which may be the case, for instance, if a spring storm deposits a lot of snow. We report normalized habitat-days because, as a spatial average, the scale is easier to conceptualize (e.g., hundred-thousands to millions of habitat-days versus <100 normalized habitat-days) and enables comparisons between regions of vastly different sizes.

To quantify total ice algal habitat extent, any pixel that met a threshold number of habitat-days during a given year was considered suitable habitat. The 7.32-day threshold in the standard run is the time needed for the ice algal population to triple at a typical light-replete growth rate (**Table 2**). The area of suitable habitat was spatially summed and normalized to the maximum ice extent of the Arctic, a given band, or a given region to obtain the proportion of suitable ice algal habitat for that area.

To examine how environmental variables related to one another, bivariate correlations between snow depth and ice thickness or age (proportion of FYI) were calculated with simple linear regressions (ordinary least squares) implemented in Python's SciPy package (Virtanen et al., 2020). A significance threshold of $p < 0.05$ was used for all statistical tests in this study. MYI was defined as any sea ice 2 years or older in the Tschudi et al. (2019) product, which

increments the age of all sea ice by 1 year on the date of the summer sea ice minimum. FYI is therefore any sea ice that forms after the summer minimum.

Time series trends with 34 annual observations were calculated with a Mann-Kendall Trend test with an accompanying Theil-Sen estimator, a non-parametric method for analyzing increasing or decreasing trends (Mann, 1945; Sen, 1968; Kendall, 1975). The Mann-Kendall test produces a p-value to indicate the significance of the trend, while the Theil-Sen estimator calculates the slope of the trend. The modifications suggested by Yue and Wang (2004) were made to account for possible serial correlation in the time series, as implemented in Python's pymannkendall package (Hussain and Mahmud, 2019).

Multiple linear regressions (ordinary least squares) were used to determine the relative importance of different physical inputs in controlling the habitat duration, quantified as normalized habitat-days. The explanatory variables considered were ice thickness, snow depth, latitude, daylength, incident light, and the bottom ice melt date, averaged spatially and temporally (January–July), for a particular year and region. Latitude was removed from the regression because it was the only explanatory variable that was insignificant and because latitude is directly related to daylength, which was already included. The remaining explanatory variables were inspected visually for linear relationships with the response variable and checked for colinearity using the variance inflation factor (VIF). VIF was <3 for all variables, indicating only moderate correlation; VIF > 5 is often considered problematic
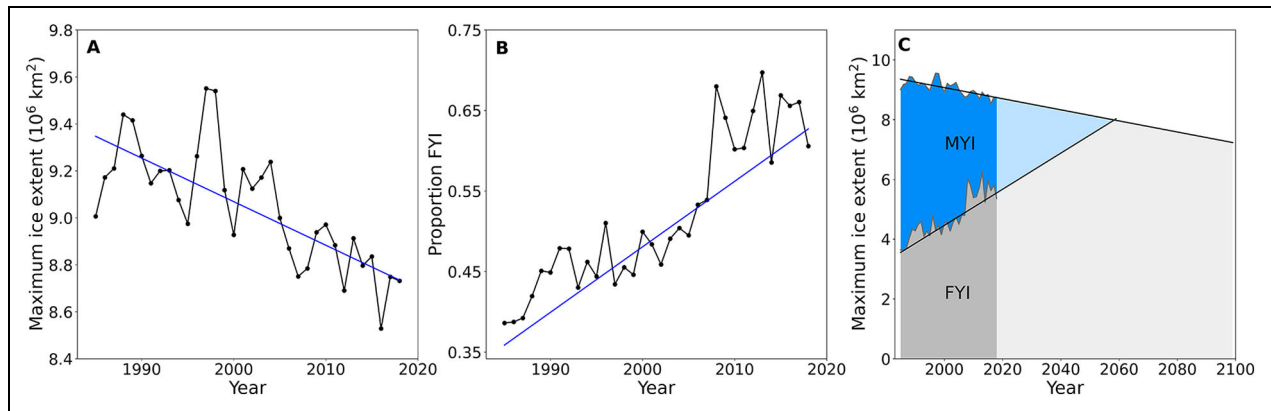
Figure 3. Trends in sea ice extent and age. Annual pan-Arctic (A) maximum sea ice extent, (B) proportion of first-year ice (FYI) during the winter maximum, and (C) maximum FYI and multiyear ice (MYI) extent projected until 2100. Trend lines indicate a significant trend based on a Mann-Kendall Trend test with an accompanying Theil-Sen slope estimate, which does not always produce the same fit as an ordinary least squares regression, but is robust for nonparametric data.

(James et al., 2013). Because the residuals versus fitted plots revealed unequal variance among groups, the response variable of normalized habitat-days was transformed by taking the square root. Residuals were also checked for normal distribution via visual inspection of quantile-quantile plots. Lastly, the relative importance of each explanatory variable was estimated by the Lindeman, Merenda, and Gold (lmg) approach, which attributes a portion of the overall regression's R^2 value to each variable (Lindeman et al., 1980). Lmg calculations were bootstrapped (1,000 replicates) to create 95% confidence intervals (CIs). All analyses related to the multiple linear regression were conducted in R, with the lmg and VIF calculations implemented in the relimpo and car packages, respectively (Grömping, 2006; Fox and Weisberg, 2019).

2.4. Sensitivity analyses

To determine the sensitivity of our assessment to different parameters, 2013 was used as a representative high habitat year and 1995 was used as a representative low habitat year. Individual parameters to assess (**Table 2**) were then varied by ±50%. The percent change from the standard run in pan-Arctic normalized habitat-days and the pan-Arctic proportion of suitable habitat was calculated for each of the 2 years. We also report the difference in habitat between the 2 years for each sensitivity run because this study emphasizes time series trends.

This study focuses on bottom ice as the major potential habitat for ice algae, which is most likely true in FYI (Leu et al., 2015; Arrigo, 2017). Some MYI cores have found peaks in ice algal biomass up to 1 m above the ice-water interface, perhaps accumulating in layers of growing ice each year or migrating vertically towards the sunlight (Gradinger, 1999; Olsen et al., 2017). We conducted an additional sensitivity analysis to estimate the contribution of interior MYI to ice algal habitat by moving the algal layer in MYI to 1 m above the ice-water interface and keeping 0.05 m in FYI.

3. Results
3.1. Sea ice and snow conditions

Above the Arctic Circle, yearly maximum sea ice extent decreased from 9.3×10^6 to 8.7×10^6 km^2 over our 34-year study (**Figure 3A**), with most variation located in the Nordic region, the Barents Sea, and, to some extent, the Kara Sea (**Table 1**). As the summer minimum ice extent decreased more rapidly than the winter maximum, FYI extent increased from 3.5×10^6 to 5.5×10^6 km^2 (**Figure 3C**). This dramatic increase from 37% to 63% FYI (**Figure 3B**) corresponded with a 0.08 m decade^{-1} decrease in average sea ice thickness (**Figure 4A**). Regionally, the proportion of sea ice that was FYI increased in all regions except the Laptev Sea, Baffin Bay, and the Nordic region. The Laptev Sea is a region that was already almost entirely (mean = 98%) FYI, while Baffin Bay and the Nordic region exhibited decreases in FYI extent that almost matched the decreases in MYI extent (Figure S1). The areas with the highest proportion of FYI also had the thinnest ice. For example, the four regions that averaged >90% FYI in 1985–2018 were the only regions with an average ice thickness <1.65 m (Baffin, Barents, Kara, and Laptev; **Table 3**). MYI was a major component of the total sea ice in some regions—the Central Basin, Chukchi Sea, Nordic region, and Siberian Sea—but based on the relative size of each region, the Central Basin was the main refuge of thick (mean = 2.28 m) MYI. The ice thicknesses reported here are averaged from January to July, and thus do not fully capture the annual cycle of sea ice growth, as described in Section 2.2. Declines in ice age and thickness were concentrated in the Central Basin and the Chukchi and Siberian seas, where trends of –0.13 to –0.14 m decade^{-1} were an order of magnitude above those in other regions.

Regional averages of snow depths on Arctic sea ice ranged from 0.067 to 0.194 m (**Table 3**). As with ice thickness, the January–July metric obscures the variation in snow depth within 1 year, with snow depth usually peaking around March or April and then rapidly dropping off in June (Stroeve et al., 2020). Snow depth was correlated positively with ice thickness (R = 0.75, n = 306
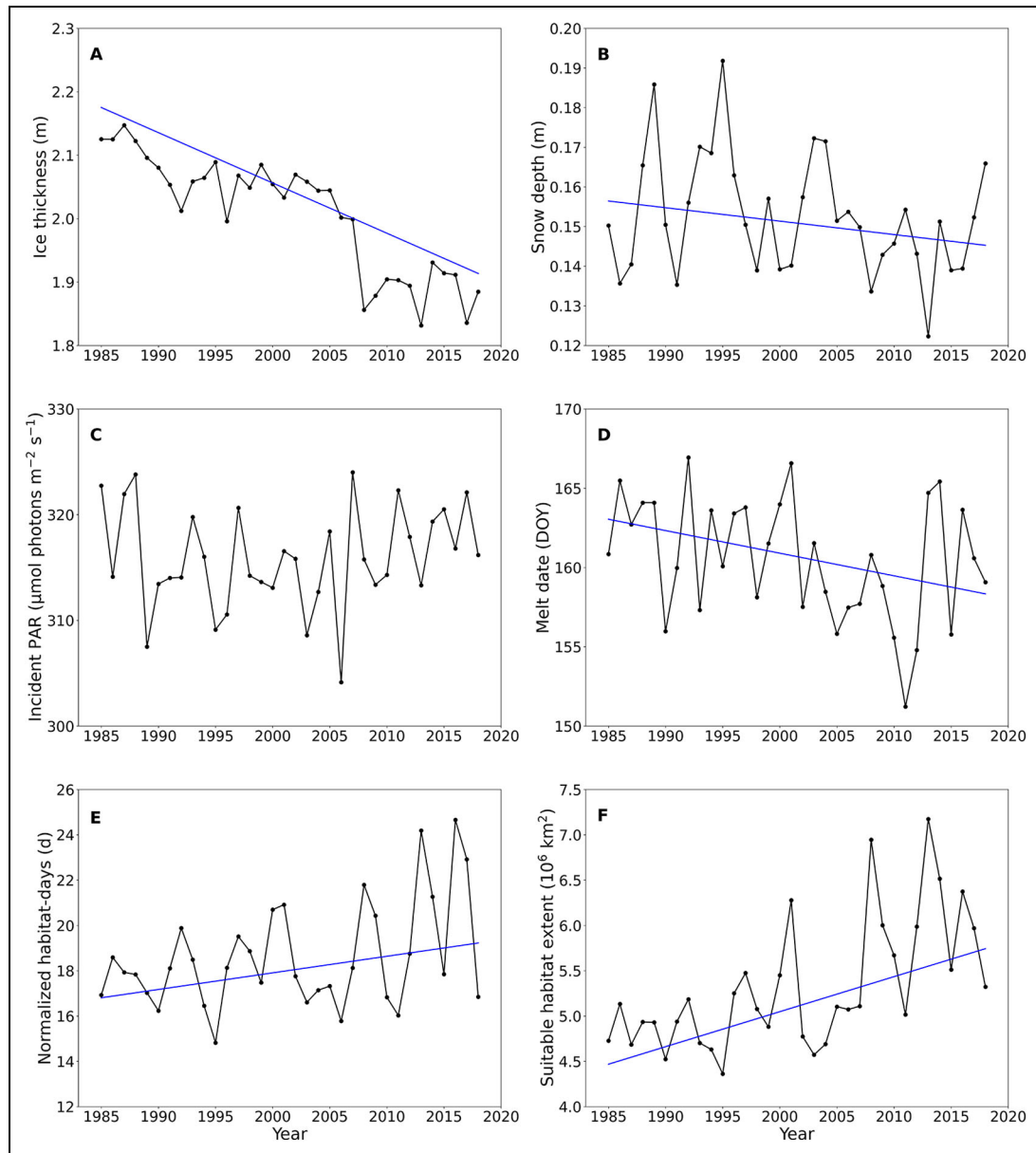
Figure 4. Trends in ice algal habitat assessment inputs and outputs. Annual pan-Arctic (A) sea ice thickness, (B) snow depth, (C) downwelling incident photosynthetically active radiation (PAR), (D) melt date reported as the day of the year (DOY), (E) normalized habitat-days, and (F) suitable habitat extent. A–C are averaged over January–July, while D–F are annual metrics. Trend lines indicate a significant trend based on a Mann-Kendall Trend test with an accompanying Theil-Sen slope estimate, which does not always produce the same fit as an ordinary least squares regression, but is robust for nonparametric data.

regions and years) and negatively with the proportion of FYI (R = −0.72, n = 306 regions and years), demonstrating how the oldest ice tends to accumulate the thickest snow cover. All regions except the Central Basin, the Beaufort Sea, and Baffin Bay saw decreasing snow depths, for a pan-Arctic rate of −0.003 m decade^{-1} (**Figure 4B**).

3.2. Atmospheric conditions
Cloud-corrected incident light increased each year during the transition from polar night to spring, and was as high as 1500 μmol photons m^{-2} s^{-1}. Though annually variable, cloud cover did not cause a notable shift in average incident light during the 34-year time series (**Figure 4C**). Four

of the regions did exhibit slight trends, with average incident light increasing in Central Basin and the Laptev Sea by 1.5 and 1.6 μmol photons m^{-2} s^{-1} decade^{-1}, respectively, and decreasing in Baffin Bay and the Barents Sea by −3.2 and −0.8 μmol photons m^{-2} s^{-1} decade^{-1}, respectively.

Air temperatures generally warmed in June, with the average melt date for all Arctic regions taking place from June 2 (DOY 153) to June 26 (DOY 177; **Table 3**). Between regions, melt dates were not related to latitude, as most of the peripheral seas had later average melt dates than the Central Basin. The Nordic region had the earliest average melt date, consistent with the melting and re-freezing

Table 3. Ice, snow, and melt conditions as means ± standard deviations (SD) and trends for January to July, 1985−2018 (n = 34)

Region	Proportion FYI		Ice Thickness		Snow Depth		Melt Date	
	Mean ± SD (prop.)	Trend (prop. decade^{-1})	Mean ± SD (m)	Trend (m decade^{-1})	Mean ± SD (m)	Trend (m decade^{-1})	Mean ± SD (DOY[a])	Trend (days decade^{-1})
Central	0.23 ± 0.14	0.11	2.28 ± 0.15	–0.13	0.194 ± 0.023	n.t.	158 ± 4	n.t.
Chukchi	0.61 ± 0.19	0.15	1.89 ± 0.18	–0.14	0.122 ± 0.032	–0.013	165 ± 6	–2.6
Beaufort	0.85 ± 0.15	0.02	1.67 ± 0.14	n.t.	0.067 ± 0.021	n.t.	165 ± 8	2.6
Baffin	0.96 ± 0.01	n.t.[b]	1.51 ± 0.06	0.04	0.088 ± 0.018	n.t.	177 ± 6	–2.3
Nordic	0.47 ± 0.09	n.t.	1.99 ± 0.09	n.t.	0.162 ± 0.039	0.012	153 ± 8	–2.3
Barents	0.91 ± 0.06	0.01	1.46 ± 0.13	n.t.	0.072 ± 0.020	–0.009	162 ± 5	n.t.
Kara	0.96 ± 0.07	0.01	1.63 ± 0.06	–0.01	0.130 ± 0.034	–0.017	163 ± 7	–2.7
Laptev	0.98 ± 0.05	n.t.	1.62 ± 0.04	n.t.	0.093 ± 0.018	–0.009	165 ± 8	–2.8
Siberian	0.68 ± 0.25	0.14	1.86 ± 0.21	–0.14	0.149 ± 0.030	–0.008	159 ± 8	–5.7
Pan-Arctic	0.52 ± 0.09	0.08	2.01 ± 0.09	–0.08	0.152 ± 0.01	–0.003	161 ± 3.8	–1.4

[a] DOY = day of the year.

[b] n.t. = no significant trend.

Table 4. Normalized habitat-days, proportion of suitable habitat, and start date as means ± standard deviations (SD) and trends for 1985−2018 (n = 34)

Region	Normalized Habitat-Days		Proportion Suitable Habitat		Start Date	
	Mean ± SD (days)	Trend (days decade^{-1})	Mean ± SD (prop.)	Trend (prop. decade^{-1})	Mean ± SD (DOY[a])	Trend (days decade^{-1})
Central	8.2 ± 3.0	2.1	0.33 ± 0.15	0.10	114 ± 7	–6.1
Chukchi	28.0 ± 7.1	1.7	0.82 ± 0.11	0.09	91 ± 8	–6.0
Beaufort	47.2 ± 8.5	2.5	0.98 ± 0.03	n.t.	82 ± 5	–1.2
Baffin	49.5 ± 7.5	–1.6	0.96 ± 0.01	n.t.	77 ± 2	1.5
Nordic	15.0 ± 3.7	n.t.[b]	0.56 ± 0.13	n.t.	91 ± 7	2.2
Barents	27.2 ± 5.4	–1.0	0.81 ± 0.08	–0.02	82 ± 4	n.t.
Kara	24.2 ± 5.8	1.4	0.90 ± 0.09	n.t.	91 ± 2	–0.9
Laptev	32.0 ± 7.5	n.t.	0.98 ± 0.04	n.t.	88 ± 2	–0.4
Siberian	19.2 ± 6.4	n.t.	0.75 ± 0.17	0.08	96 ± 9	–4.8
Pan-Arctic	18.6 ± 2.3	0.7	0.59 ± 0.09	0.05	100 ± 4	–3.1

[a] DOY = day of the year.

[b] n.t. = no significant trend.

frequently seen in the sea ice data in that region (Tschudi et al., 2019). Six regions trended towards earlier melt dates by 2–3 days decade^{-1}. The exceptions are the Central Arctic and the Barents Sea, which both featured no trend in melt dates, and the Beaufort Sea, which trended towards later melt dates (2.6 days decade^{-1}; **Table 3**). The Siberian Sea featured the most dramatic shift to earlier melt dates at a rate of 5.7 days decade^{-1}. Over the 34-year time series, the average pan-Arctic melt date shifted from June 12 (DOY 163) to June 7 (DOY 158; **Figure 4D**).

3.3. Ice algal habitat-days

Arctic sea ice first supported net positive ice algal photosynthesis in mid-March and April, transmitting enough light as early as March 18 (DOY 77) in Baffin Bay and as late as April 24 (DOY 114) in the Central Arctic (**Table 4**).
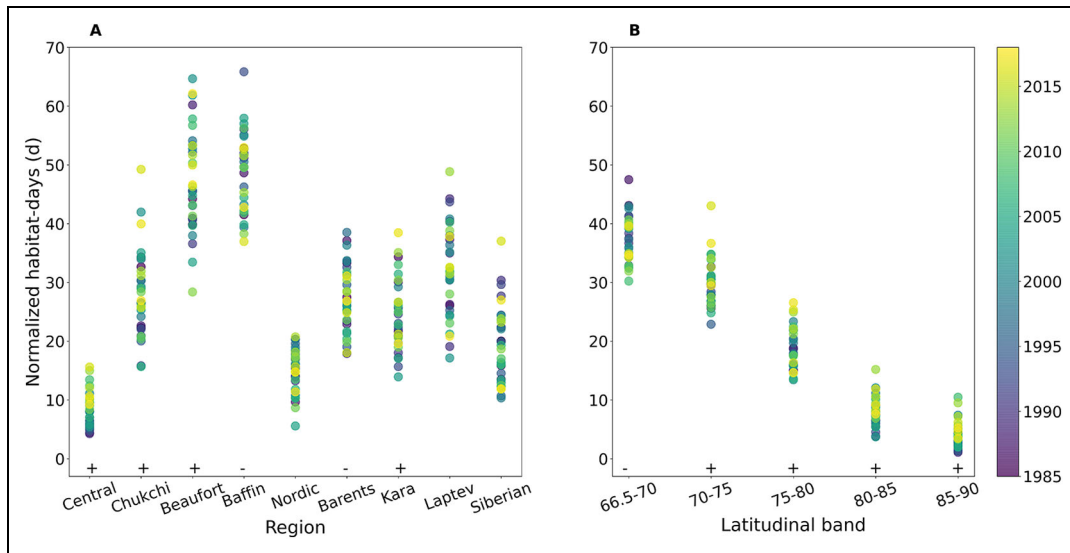
Figure 5. Normalized ice algal habitat-days. Ice algal habitat-days are normalized to a given (A) region or (B) latitudinal band, colored by year. Significant increases (+) and decreases (–) over time are marked above the x-axis.

Across the Arctic, the start of ice algal growth shifted earlier by 3.1 days decade^{-1}, but this was largely driven by 1.5 to 2 times greater trends in the Central Basin and the Chukchi and Siberian seas. In contrast, the timing of sufficient light transmission in Baffin Bay and the Nordic region trended in the opposite direction, and between 1985 and 2018, sea ice started to support ice algae later in the year.

The metric of normalized habitat-days represents the spatially-averaged duration of ice algal habitat. Due to its nature as a spatial average, this metric is not necessarily congruent with the number of days between the start and melt dates for each region. The range in the average number of normalized habitat-days among the different regions was large, with the smallest being 8.2 days in the Central Arctic and the largest being 47.2 days and 49.5 days in the Beaufort Sea and Baffin Bay, respectively (**Figure 5A**; **Table 4**). When divided into 5° latitudinal bands, an almost stepwise relationship between normalized habitat-days and latitude was observed, with the least habitat at higher latitudes (**Figure 5B**). There was a fair degree of interannual variability in normalized habitat-days, with pan-Arctic values rising or falling by up to 36% (average difference of 2.1 days) from year to year. Over the 34-year time series, regional trends in normalized habitat-days differed in both direction and magnitude, with 1.4–2.5 days decade^{-1} increases in the Central Basin and the Chukchi, Beaufort, and Kara seas and 1.0–1.6 days decade^{-1} decreases in the Barents Sea and Baffin Bay, respectively (**Figure 5A**; **Table 4**). Normalized habitat-days increased in each latitudinal band, except for a decrease in the southernmost band (66.5–70°N; **Figure 5B**). On a pan-Arctic scale, this increase translates to the average ice algal growth season lengthening by 2.4 days over the 34-year period (**Figure 4E**). When related to ice age, both regions and latitudinal bands with a greater proportion of FYI had more normalized habitat-days (**Figure 6A** and **C**; R = 0.64 for regions and R = 0.93 for latitudinal bands).

A multiple linear regression explained 91.7% of the variance in the square root of normalized habitat-days between Arctic regions using ice thickness, snow depth, daylength, incident light, and melt date as predictors. Snow depth was the most important predictor, explaining 28.1% of the variance in the square root of normalized habitat-days. Ice thickness and melt date were the next most important and were statistically indistinguishable, explaining 21.7% and 22.4% of the variance, respectively. Lastly, incident light accounted for 16.0% and daylength accounted for 3.4% of the variance. Separate multiple linear regressions using the same predictor and response variables were conducted for each region. The best predictor was quite variable among regions: snow depth was the most important in Baffin Bay and the Chukchi, Beaufort, and Kara seas, melt date was the most important in the Nordic region and the Laptev and Siberian seas, ice thickness was the most important in the Central Basin, and incident light was the most important in the Barents Sea. Confidence intervals and more details on the multiple linear regressions are reported in Table S1.

3.4. Suitable ice algal habitat extent

The area of suitable habitat, which we defined as supporting at least a tripling in the initial ice algal population, increased from 4.4×10^6 to 5.7×10^6 km^2 (**Figure 4F**) or from 48% to 66% of sea ice above the Arctic Circle between 1985 and 2018. The 0.4×10^6 km^2 decade^{-1} rate of increase in suitable habitat was twice the rate of Arctic sea ice loss. This trend emerges despite average interannual differences of ±6% suitable habitat. Four regions (Beaufort, Baffin, Kara, Laptev) were ≥90% suitable on average and did not experience any change over the time series (**Table 4**; **Figure 7A**). Of the five remaining regions that were <90% suitable on average, three (Central, Chukchi, Siberian) exhibited positive trends in the proportion of suitable habitat, while the Barents Sea was the only region where suitable habitat decreased (–0.02 decade^{-1}).
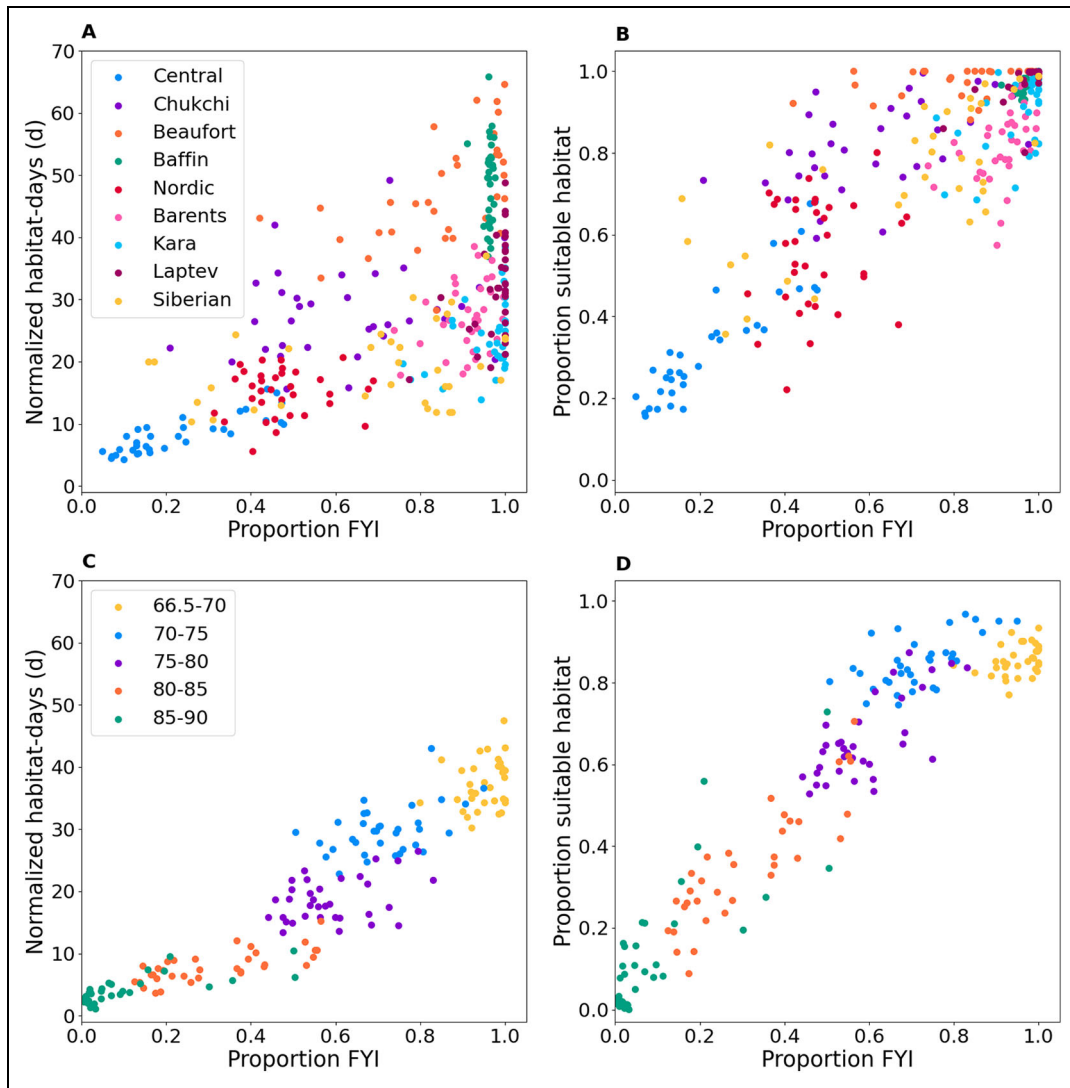
Figure 6. Correlation between the proportion of first-year ice and ice algal habitat. The proportion of sea ice that is first-year ice (FYI) is shown for each year and (A and B) region or (C and D) latitudinal band. Ice algal habitat is quantified by (A and C) pan-Arctic normalized habitat-days and (B and D) the proportion of the Arctic that is suitable habitat.

The Nordic region stands out as the region with some of the least suitable habitat—56% on average and second only to the Central Basin (33% suitable)—yet it showed no trend. Notably, only the Central Basin and the Chukchi Sea featured positive trends in both normalized habitat-days (2.1 and 1.7 days decade^{-1}, respectively) and the proportion of suitable habitat (0.10 and 0.09 decade^{-1}, respectively). When divided into latitudinal bands, a nearly stepwise relationship was again observed, where higher latitudes had less suitable habitat (**Figure 7B**). However, higher latitude bands also had a wider range in the proportion of suitable habitat during the study period; for example, the 85–90°N band was anywhere from 0 to 73% suitable, depending on the year. All latitudinal bands except 66.5–70°N had a positive trend in the proportion of suitable habitat. The influence of ice age on habitat extent was similar to that on normalized habitat-days: the greater the proportion of FYI in either a region or latitudinal band, the higher the proportion of suitable habitat (**Figure 6B** and **D**; R = 0.86 for regions and 0.94 for latitudinal bands).

3.5. Sensitivity analyses

Our assessment was moderately sensitive to parameter variations of ±50%, and more so with respect to pan-Arctic normalized habitat-days than the proportion of suitable habitat (**Table 5**). The assessment was the most sensitive to R and the K_d of interior ice, which were the only parameters to induce >50% changes in both habitat metrics and in the difference between the low habitat year (1995) and high habitat year (2013). Varying the K_d of dry snow and α also increased the difference in normalized habitat-days between 1995 and 2013 by >50%, but had a smaller effect on the other metrics. Moving the algal layer in MYI from 0.05 m to 1 m above the ice-water interface results in a 5% increase in light transmission to the algal layer, based on the value used for the K_d of interior ice (**Table 2**). The addition of interior communities in MYI then increased the proportion of suitable habitat by up to 57.5% of the control run for the entire Arctic (**Table 5**). Most importantly, while the magnitude of the difference between the years did vary, the direction of
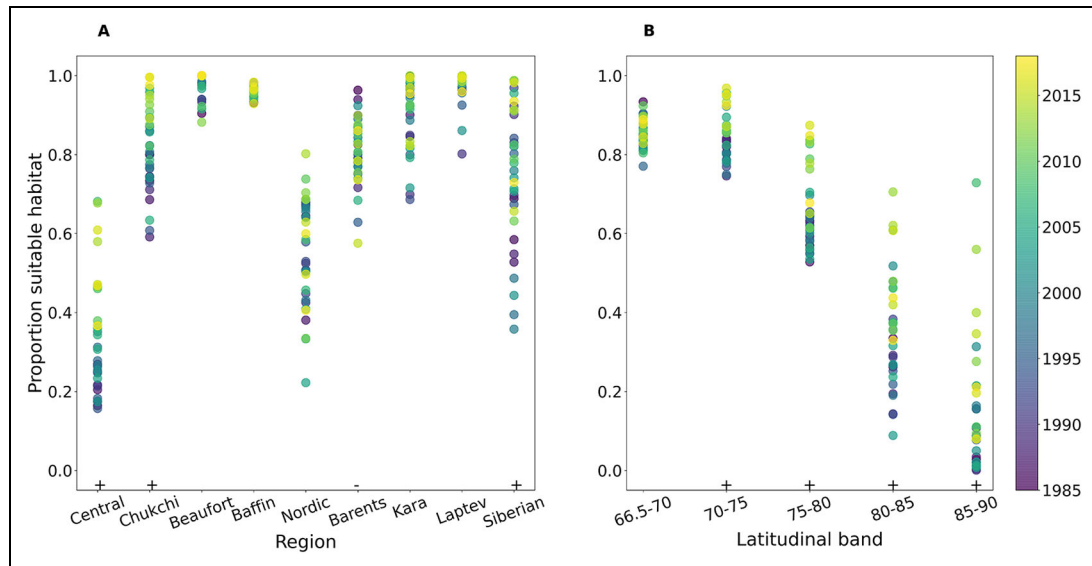
Figure 7. Proportion of suitable ice algal habitat. Proportion of a given (A) region and (B) latitudinal band that is suitable ice algal habitat, colored by year. Significant increases (+) and decreases (−) over time are marked above the x-axis.

difference was always the same. That is, 2013 always maintained a greater extent and longer duration of habitat compared to 1995.

4. Discussion

In this study, we quantified Arctic bottom ice algal habitat and its response to climate change at larger spatial (pan-Arctic) and longer temporal (1985–2018) scales than previously reported. Thirty-four years of sea ice observations were used to calculate radiative transfer to the ice algal layer. In particular, we leveraged the length of the sea ice age record, an approach which is distinct from other observation-based studies that are constrained to shorter periods (e.g., Lange et al., 2017; Stroeve et al., 2021) and from studies that use Earth system models to represent sea ice growth (e.g., Watanabe et al., 2019). The new metric of (normalized) habitat-days was developed to jointly assess ice algal habitat duration and extent in the face of high temporal and spatial variability. The metric of suitable habitat extent (or proportion) is used to report a more intuitive measurement of the spatial dominance of ice algal habitat. Overall, we assessed the balance between the decrease in Arctic ice extent, which is expected to be detrimental to ice algae, and the replacement of MYI with optically thinner FYI, which is expected to favor ice algae. Our study finds that: 1) approximately half of Arctic sea ice is suitable ice algal habitat, with snow depth, the date of bottom ice melt, and ice thickness acting as the primary drivers of habitat extent and duration; 2) habitat increased in extent and duration between 1985 and 2018 due to the increase in FYI; and 3) the annual timing of habitat has shifted to earlier in the spring. Below we discuss these findings and the implications for the continually melting sea ice environment in the Arctic Ocean.

4.1. Status and drivers of Arctic ice algal habitat

According to our habitat assessment for 1985–2018, 48–66% of Arctic sea ice north of 66.5°N is suitable habitat for bottom ice algae in spring. To our knowledge, Lange et al. (2017) is the only other study to provide an estimate of ice algal habitat extent in the Arctic, by identifying a threshold light transmittance for ice algal growth, calculating the transmission through five categories of ice type/snow cover, and then applying the resulting categories to remotely sensed sea ice and snow. Our estimates are in line with their finding that 65% of ice was suitable habitat in April 2013, although their study domain differed slightly (i.e., the present study includes Baffin Bay and other lower latitude ice). The spatial patterns of ice algal habitat are also comparable, with both studies finding the area north of the Canadian Arctic the least suitable, due to the persistence of thick MYI (**Figure 2**; Lange et al., 2017). However, we were also able to assess the temporal evolution of ice algal habitat, both within each year and over the 34-year time series.

Of the factors included in this assessment, snow depth was the primary driver of regional and interannual variation in normalized habitat-days. A snow cover that is too thick will not transmit enough light to support ice algal growth, even though ice algae are extremely low-light adapted and the compensation irradiance for ice algae is estimated to be 0.17–10 μmol photons m^{-2} s^{-1} (Horner and Schrader, 1982; Cota, 1985; Gosselin et al., 1985; Gosselin et al., 1986; Mock and Gradinger, 1999; Hancke et al., 2018). Snow is optically thick; for example, according to our radiative transfer model, 47 μmol photons m^{-2} s^{-1} of an incident irradiance of 390 μmol photons m^{-2} s^{-1} (example from noon on May 15, 2000) would be transmitted through a 0.1-m snow cover to the snow-ice interface. By the time the light reaches the algal layer through 1.5 m of ice, only 3 μmol photons m^{-2} s^{-1} would remain. Therefore, because snow has such a high K_d (**Table 2**),

Table 5. Sensitivity analysis for 1995 (low ice algal habitat year) and 2013 (high ice algal habitat year)

Parameter[a]	Treatment	Normalized Habitat-Days			Proportion Suitable Habitat		
		% Change 1995	% Change 2013	Diff. 2013–1995[b]	% Change 1995	% Change 2013	Diff. 2013–1995[b]
Standard run	N/A[c]	N/A	N/A	9.4	N/A	N/A	0.32
P_{max}	+50%	11.6	11.2	10.4 (+1.0)	6.1	2.7	0.31 (–0.01)
	–50%	–43.5	–43.0	5.4 (–4.0)	–31.2	–20.8	0.30 (–0.02)
α	+50%	30.6	28.9	11.8 (+2.4)	20.8	11.6	0.31 (–0.01)
	–50%	–46.5	–48.1	**4.6 (–4.8)**	–38.1	–34.8	0.22 (–0.10)
Respiration rate	+50%	–45.0	–45.6	5.0 (–4.4)	–34.8	–28.3	0.26 (–0.06)
	–50%	**73.2[d]**	**67.2**	14.8 (+5.4)	**51.2**	19.2	0.22 (–0.10)
Scattering layer thickness	+50%	–25.2	–25.3	7.0 (–2.4)	–19.2	–12.8	0.31 (–0.01)
	–50%	27.3	25.9	11.6 (+2.2)	18.2	10.3	0.31 (–0.01)
Diffuse attenuation coefficient of dry snow	+50%	–22.1	–24.1	6.8 (–2.6)	–16.2	–11.6	0.30 (–0.02)
	–50%	47.6	49.5	**14.3 (+4.9)**	29.9	14.9	0.29 (–0.03)
Diffuse attenuation coefficient of scattering ice	+50%	–37.7	–38.3	5.7 (–3.7)	–29.6	–23.7	0.27 (–0.05)
	–50%	41.7	38.9	12.6 (+3.2)	29.3	14.8	0.29 (–0.03)
Diffuse attenuation coefficient of interior ice	+50%	**–56.4**	**–59.2**	**3.4 (–6.0)**	–49.6	**–53.5**	**0.13 (–0.20)**
	–50%	**77.4**	**63.3**	13.2 (+3.8)	**77.5**	20.9	**0.10 (–0.22)**
Melt date threshold	+50%	26.0	13.7	8.8 (–0.6)	10.5	6.7	0.32 (0.00)
	–50%	–28.3	–24.1	7.7 (–1.6)	–20.7	–9.9	0.34 (+0.02)
Freeze-up threshold	+50%	6.08	7.0	10.2 (+0.8)	4.4	1.4	0.31 (–0.01)
	–50%	–0.5	1.5	9.8 (+0.4)	0.4	0.7	0.32 (0.00)
Suitable habitat threshold	+50%	N/A	N/A	N/A	–16.0	–10.4	0.31 (–0.01)
	–50%	N/A	N/A	N/A	26.6	14.1	0.30 (–0.02)
Algal layer location	+50%	2.1	2.2	9.6 (+0.2)	1.6	0.9	0.32 (0.00)
	–50%	–2.3	–2.2	9.2 (–0.2)	–1.6	–0.9	0.32 (0.00)
MYI algal layer location[e]	0.05 to 1.0 m	34.1	17.1	8.5 (–0.9)	**57.5**	16.4	**0.14 (–0.18)**

[a] P_{max} = maximum photosynthetic rate; α = the slope describing the relationship between irradiance and photosynthetic rate before light-saturation.

[b] Difference between years for the habitat metrics, with the direction and magnitude of change relative to the standard run in parentheses.

[c] N/A = not applicable.

[d] Bold indicates changes >50%.

[e] Algal layer in multiyear ice (MYI) moved from 0.05 to 1.0 m above the bottom of the ice (ice-water interface).

even minor variations in snow depth, which usually span a range of 0–1 m, greatly alter the light available to ice algae. Several other studies have similarly found that snow depth plays a key role determining springtime under-ice light fields (Stroeve et al., 2021) and ice algal bloom initiation (Welch and Bergmann, 1989; Bergmann et al., 1991; Rysgaard et al., 2001; Leu et al., 2015).

Although light attenuation (per meter) by sea ice is much less than that by snow, ice thickness was almost as important as snow depth in determining ice algal habitat and extent. Its effect is clearly seen in the relationships between the proportion of FYI and both normalized habitat-days and the proportion of suitable habitat (**Figure 6**), where regions and latitudinal bands with a greater proportion of FYI are marked by thinner ice that transmits more light. Sea ice age is also known to affect snow depth, primarily because MYI can accumulate snow early in the fall before the formation of FYI (Blanchard-Wrigglesworth et al., 2015; Liston et al., 2020), and a negative correlation between snow depth and the proportion

of FYI is confirmed in our analysis. Therefore, there is a compounding effect where FYI both is thinner and generally supports a thinner snow cover, making it even more conducive for ice algal growth.

The timing of bottom ice melt was another important variable in explaining the variation in normalized habitat-days. As the Arctic moves from winter into spring, both light intensity and daylength (photoperiod) increase. Melting later in the year increases the chance that the transmitted light will be sufficient to support net ice algal growth. Similarly, the later the melt, the longer the ice algal habitat can persist. Demonstrating how earlier melt dates truncate the growing season, the Nordic region had the earliest average melt dates (**Table 3**) and was one of the regions where melt date was the most important predictor of normalized habitat-days. Daylength was a relatively minor predictor in the multiple linear regression because it does not vary interannually, but it is an important factor seasonally.

Our sensitivity analyses demonstrate that the direction of trends in normalized habitat-days and the proportion of suitable habitat reported here remain the same when parameter values are varied. Given that snow depth and ice thickness were among the top controls of normalized habitat-days, it is not surprising that the sensitivity analysis highlighted the K_d of interior ice, and to some extent, the K_d of dry snow, as important parameters. As either of these K_d values increases, the light available to ice algae rapidly diminishes. The sensitivity analysis also identified R, algal respiration, as important to both normalized habitat-days and the proportion of suitable habitat. R offsets photosynthetic carbon fixation, and therefore alters the amount of light required for net positive growth. The values of K_d and R are taken directly from published field measurements (Perovich et al., 1986; Suzuki et al., 1997), and so the uncertainty around these parameters is unlikely to be as high as the $\pm 50\%$ variation tested in our sensitivity analysis. In contrast, the three parameters that were designed for this study and thus are poorly constrained were among the least sensitive parameters: the thresholds for melt date, freeze-up, and suitable habitat. Overall, our study design leverages known ice algal characteristics to determine the circumstances that support ice algae. Moving the MYI algal layer to 1 m above the ice-water interface also notably increased the proportion of suitable habitat, indicating that our focus on bottom ice may underestimate total habitat. The magnitude of underestimation depends on factors that are even less understood for interior ice, such as nutrient delivery to and algal photophysiology within interior communities. Adding interior MYI as potential habitat did not change our larger finding that 1995, which had 56% MYI, featured less ice algal habitat than 2013, which had 30% MYI (**Table 5**). MYI remains a less favorable habitat than FYI because its thick layer of snow transmits so little light.

Some simplifications were necessary to represent how the snow and sea ice environment affect Arctic ice algal habitat. For one, the bottom ice melt was determined solely by air temperatures and did not vary under different snow and sea ice conditions. In reality, how rapidly the sea ice warms in response to atmospheric forcing depends on the snow cover, ice thickness, and ice algal biomass. As air temperatures in spring begin to warm, a deep snow cover minimizes heat transfer to the ice and can delay bottom ice melt and ice algal release (Mundy et al., 2005; Juhl and Krembs, 2010; Campbell et al., 2015; Hancke et al., 2018). Thicker ice may similarly delay bottom ice melt, as transmission of heat to the bottom layer takes longer in thicker ice. In support of this effect, ice thickness has correlated positively with ice algal bloom duration in some ecosystem models (Watanabe et al., 2019). Under an extremely thin snow cover (<0.05 m), local heating of the bottom ice as ice algae convert PAR to heat can hasten ice melt (Zeebe et al., 1996). In all three cases, including the effects of snow and ice as thermal insulators may increase our estimates of normalized habitat-days in areas with thick snow and ice, such as the Central Arctic, but decrease our estimates in areas with thin snow and ice, such as Baffin Bay and the Beaufort, Barents, and Laptev seas. If we assume, for example, that each additional 0.01 m of snow delays bottom ice melt by up to 1 day (Grossi et al., 1987; from data published in Campbell et al., 2015), our estimate of normalized habitat-days would change by approximately $\pm 15\%$.

Another simplification in our habitat assessment was the use of a single snow texture and a uniform icescape, which may underestimate light availability. We used a single K_d value for dry snow, while snow metamorphosis (restructuring and reshaping of the snow crystal/grain) over a season has been proposed to alter snow optical properties enough to enable ice algal growth under a thick snow cover in Greenland (Hancke et al., 2018). However, as snow metamorphosis is tied to warming air temperatures, it would likely add only a few days of ice algal growth to our estimates before the bottom ice melts. We also assumed a uniform ice thickness and icescape in each 12.5 km pixel, but ice age and type may have an even greater influence on habitat suitability due to features like hummocks and leads. MYI hummocks tend to have little snow (<0.2 m) because they protrude above the adjacent ice, thereby increasing the light that penetrates to the bottom ice (Lange et al., 2017). Snow distribution surveys in the Lincoln Sea (Central Arctic) suggest that hummocks may be a feature in up to 15% of MYI (Lange et al., 2015). Meanwhile, open and refrozen leads tend to form in thinner, more dynamic ice environments and also allow greater light transmission (Kauko et al., 2017). However, under-ice or ice-edge phytoplankton, rather than ice algae, may benefit more from increased light through leads (Assmy et al., 2017; Kauko et al., 2017), as lead formation is most associated with the start of sea ice breakup. Altogether, ice algal habitat may respond even more dramatically to the changing snow and ice environment than represented here.

4.2. Habitat trends and implications for net primary production

To understand the forces changing the Arctic sea ice environment, examining the two atmospheric reanalyses employed in this study is useful. The snow depth estimates from SnowModel-LG were forced by ERA5, while the

Gregg and Carder (1990) atmospheric radiative transfer model and our melt date analysis used NCEP/NCAR Reanalysis 1. Both ERA5 and NCEP/NCAR show strong warming trends over the Arctic, with the most severe changes above the Central Arctic (Francis et al., 2017; Overland et al., 2018; You et al., 2021). As air temperatures increased by 0.72°C decade^{-1} (1979–2020; You et al., 2021), local sea ice melt caused by Arctic warming was a major, though not the only, contributor to the observed declines in sea ice extent, thickness, and age (Stroeve and Notz, 2018). Additional intertwined factors include the export of sea ice out of the Arctic, self-amplification of ice loss through the ice-albedo feedback loop, changing ocean and atmospheric circulation patterns, and a positive Arctic Oscillation in the 1980s–1990s (Stroeve and Notz, 2018). The thinning snow cover over much of the Arctic Ocean is attributable to the decreased accumulation on FYI over a shorter sea ice season, not to any long-term trends in precipitation (Barrett et al., 2020; Stroeve et al., 2021).

As a result of the physical changes in the Arctic, sea ice became a more favorable environment for ice algae in spring over the 1985–2018 study period. Ice algal habitat increased when measured both as normalized habitat-days and as the proportion of suitable habitat. The rate of habitat expansion outpaced the rate of winter ice loss, overpowering any negative effect due to the overall decrease in Arctic sea ice extent. Instead, the replacement of MYI with FYI promoted habitat expansion. We attribute this pattern to an increase in light transmission through thinner snow and thinner, younger ice. Trends in the bottom ice melt date cannot explain an increase in ice algal habitat, as the shift towards earlier melt dates actually decreases habitat, likely dampening the effects of thinner snow and ice. Neither is changing cloudiness over the Arctic Ocean likely to explain the large increase in ice algal habitat, as trends in incident light were small in magnitude. Taking the Central Basin as an example, the 5.1 μmol photons m^{-2} s^{-1} increase over 34 years equals a 1.7% increase in incident light, compared to a 29% decrease in ice thickness. The multiple linear regression also revealed that, of the variables considered, incident light explained the least amount of regional and interannual variance in normalized habitat-days. Thus, we conclude that the decreased snow depth and ice thickness, which are both related to a greater proportion of FYI, are the primary causes of increased ice algal habitat duration and extent.

Taken together, the increase in habitat duration and extent strongly suggest that net primary production in Arctic sea ice has also increased over the last three and a half decades; ice algae are likely fixing carbon over a larger area for a longer period of time. This increase in production has been predicted in several other studies with regards to the future Arctic Ocean. Based on a general understanding of the sea ice ecosystem, Leu et al. (2015) suggested that a larger proportion of FYI and thinner snow will increase ice algal blooms in the future. Tedesco et al. (2012) modeled higher ice algal production off the Greenland coast under a mild climate change scenario (2071–2090), and Tedesco et al. (2019) modeled higher ice algal production under Climate Model Intercomparison Project (CMIP)5 forcings (2061–2100), particularly above 74°N due to the gain of FYI. We attribute the ice algal habitat increase in our study to similar drivers, but this study is one of the first to demonstrate that this change is not just a future prospect but has already been taking place on a large scale in the rapidly melting Arctic Ocean. The possibility of a large-scale increase in production is supported by a recent one-dimensional ecosystem modeling study, which found that ice algal production on the Chukchi shelf increased by 0.05 g C m^2 yr^{-1} over a similar time period (1988–2018; Payne et al., 2021). However, ice algal production estimates (1980–2009) from five pan-Arctic ecosystem models are less clear, despite agreement that ice thickness and snow depth decreased significantly across the Arctic (Watanabe et al., 2019). Between these ecosystem models, there were no trends in ice algal production in the Chukchi Sea and the Barents Sea, two negative trends in the Canada Basin, and two negative and one large positive trend in the Eurasian Basin. A major source of intermodel differences was the value chosen for the maximum ice algal growth rate (0.85–4.0 d^{-1}), which controls peak biomass. Ice algal biomass was strongly correlated with ice algal production (Watanabe et al., 2019), highlighting a chain of connections that may demonstrate the advantages of the approach taken in our study—minimizing the need to accurately represent biological processes and taking maximum advantage of satellite observations of sea ice.

For increased ice algal habitat to result in increased primary production, we must assume that all sea ice is able to be colonized by ice algae and that surface nutrients throughout the Arctic are sufficient to support ice algal growth. Successful colonization depends on a sufficient seed population of algae from the sediments, the water column, or neighboring MYI (Garrison et al., 1983; Gradinger and Ikävalko, 1998; Różańska et al., 2008; Olsen et al., 2017; Kauko et al., 2018). The survival of a seed population is most challenging in the Central Arctic, where sediments are extremely deep (about 4,000–4,500 m) and lower light and nutrients are less likely to support pelagic growth. Because ice algae have historically been found across the Central Arctic once environmental conditions are favorable (Gosselin et al., 1997; Gradinger, 1999; Melnikov et al., 2002), seeding material is not likely to be limiting, especially at the large 12.5-km scale considered here. With regards to nutrient availability, there is likely sufficient nitrogen—the limiting nutrient in the Arctic (Tremblay et al., 2015; Randelhoff et al., 2020)—throughout the upper Arctic Ocean to sustain bottom ice algal production for the entire bloom. Back-of-the-envelope calculations demonstrate that maximum ice algal biomass of 350 mg Chl *a* m^{-2} in the peripheral seas and 10 mg Chl *a* m^{-2} in the Central Basin (Arrigo, 2017) are unlikely to exhaust winter surface nitrate concentrations of 10–15 and 1–5 μmol L^{-1}, respectively (Zhang et al., 2010; Randelhoff et al., 2020), if the mixed layer depth is at least 5–10 m. The most likely cause of nutrient limitation of ice algal growth is not a nutrient reservoir that is too small, but rather, limited nutrient fluxes into the sea ice. The

dominant mechanism of desalination in sea ice is gravity drainage, wherein cold, saline brine is rejected during sea ice growth and is replaced by less dense seawater (Notz and Worster, 2009). The resulting exchange is the major process supplying new nutrients to algae in the brine network (Meiners and Michel, 2017). Similar convection caused by the growth of the bottom skeletal ice layer (Wakatsuchi and Ono, 1983) is a source of nutrients to ice algae at the ice-ocean interface. The close ties between ice growth and nutrient fluxes imply that nutrient replenishment slows dramatically or stops when sea ice stops growing. In our study, we also consider this period to be the end of the ice algal bloom, when cells slough off the melting bottom ice. Therefore, the conditions under which ice algae are most likely to experience nutrient stress are not considered habitable by our metrics.

While trends in sea ice extent and thickness, snow depth, melt date, and the extent and duration of ice algal habitat are significant on a pan-Arctic scale, they tend to be highly localized. The Central Basin and the Chukchi Sea were the only regions that exhibited increases in both normalized habitat-days and the proportion of suitable habitat over our 34-year study. Increased habitat in the Chukchi Sea can be explained by the fact that the Chukchi Sea experienced some of the sharpest declines of the entire Arctic in both ice thickness and snow depth—1.8- and 4.3-fold greater than the pan-Arctic trends, respectively. Ice thickness decreased at a similar rate in the Siberian Sea and snow depth decreased even more rapidly in the Kara Sea, but neither experienced both rapid snow and ice decline as in the Chukchi Sea. In contrast, while it featured no trend in snow depth, the Central Basin was the region most affected by declining ice thickness (the most important predictor in the multiple linear regression for the Central Basin). Composed of 39% MYI in 1985, sea ice in the Central Basin was simply too thick to transmit much light. The rapid gain of FYI transformed the region into one with more prolonged and widespread ice algal habitat. Given that it is an order of magnitude larger in size than the other regions, the increased ice algal habitat in the Central Basin is largely, though not entirely, responsible for the trends observed on the pan-Arctic scale. Lastly, the Barents Sea was the only region where both normalized habitat-days and the proportion of suitable habitat decreased over 1985–2018, despite a thinning snow cover. We attribute the loss of habitat to concurrent decreases in FYI and MYI extent (Figure S1).

4.3. Ice algal habitat phenology

The timing of ice algal growth is particularly important because it is the first pulse of seasonal production in the Arctic Ocean. Although ice algal biomass is not modeled here, we can assess its phenology based on the start of net positive ice algal growth and bloom termination (the start of bottom ice melt). Start dates of mid-March to mid-April are similar to field-derived estimates (Leu et al., 2015). The average start date of April 24 in the Central Arctic (the latest of all regions due to the delayed emergence from polar night) in our study is within 1 week of the

approximate start date from the SHEBA ice camp in the Canadian Basin (Leu et al., 2015). Most Arctic ecosystem models are also comparable to our study, with ice algal blooms generally starting in March and peaking around mid-April to mid-May (Jin et al., 2012; Ji et al., 2013; Watanabe et al., 2019). We note that modeled ice algal phenology is highly variable, with interannual fluctuations as large as 2 months in a single model (Watanabe et al., 2019), which makes comparisons difficult. With that being said, several models have ice algal blooms in the Chukchi Sea starting in February (Watanabe et al., 2015; Zhang et al., 2015, as run in Watanabe et al., 2019), 4–6 weeks earlier than in our study. Likewise, based on a compensation irradiance of 0.17–5.0 µmol photons m^{-2} s^{-1}, Stroeve et al. (2021) estimated that there is sufficient light transmission to support ice algal growth in much of the Arctic by February. These earlier dates may be explained by their use of compensation irradiance as the singular threshold for ice algal growth, which only accounts for light intensity, not photoperiod. Our study incorporates both light intensity and photoperiod by calculating net Chl a-specific photosynthesis every 3 h, then integrating over a full day. We found that daylight hours in February are simply too short for gross photosynthesis to offset respiration.

Concurrent snow and bottom ice melt, causing ice algae to slough off the ice, began around June 2–26 across the Arctic. In Baffin Bay, snow melt and ice algal decline at the Green Edge ice camp started on June 3 and 8, in 2016 and 2015, respectively (Oziel et al., 2019). Likewise, in the Chukchi Sea, ice algae were found as late as June 17 in 2014 but were virtually nonexistent by the start of a 2010 cruise in which the first ice core was taken on June 22 (Selz et al., 2018). A singular event that releases all ice algae from the sea ice is unlikely, as sediment traps in the Chukchi Sea have captured fluxes of sympagic diatoms as early as February (Lalande et al., 2020). There may be a seasonal succession where different sympagic species dominate the ice and the ensuing water column fluxes at different points in the spring (Lalande et al., 2020). However, our parameterization for the end of spring ice algal habitat is in line with the large scale patterns of bottom ice melt.

Sea ice started to support ice algae earlier in the year during our study period (10.5-day pan-Arctic average over 1985–2018), but warm air temperatures also caused earlier termination of ice algal blooms (by 2.8 days). A similar shift is also represented in Arctic ecosystem models where ice algal blooms are peaking earlier by 1–3 days $decade^{-1}$ (Watanabe et al., 2019), a trend that is predicted to continue under future climate conditions (Tedesco et al., 2019). Due to the tight temporal coupling between Arctic primary producers and grazers, earlier ice algal blooms may affect the Arctic food web. Some Arctic zooplankton consume a diet primarily of ice algae early in the year (Runge and Ingram, 1988; Søreide et al., 2010; Durbin and Casas, 2014) before the development of under-ice or open water phytoplankton blooms, which lag behind ice algal blooms by 28–90 days (Ji et al., 2013; Payne et al., 2021). Whether grazers have or will be able to adapt to the changes in ice algal timing is unknown, particularly in the

case of copepods (e.g., *Calanus* spp.) with overwintering dormancy strategies and long life cycles (Conover, 1988; Falk-Petersen et al., 2009; Søreide et al., 2010). If grazers are unable to adapt, a resulting trophic cascade may affect higher pelagic trophic levels (Post, 2017), while more ice algal biomass may be exported to the deep ocean and the benthos (Ambrose et al., 2005; Renaud et al., 2007; Boetius et al., 2013). In the scope of the Arctic marine carbon cycle, the magnitude of these potential changes is relatively small, yet these shifts in timing may favor certain higher trophic level species or alter the nature and timing of organic matter export.

4.4. Future implications
Under the current climate trajectory, the Arctic Ocean will almost certainly continue to experience severe and rapid changes to the sea ice environment. We expect that Arctic sea ice will become more favorable for ice algae as the remaining one-third of Arctic sea ice that is MYI (Kwok, 2018) is replaced by FYI. The Central Arctic and the Nordic region were the only regions that still had a large proportion (>15%) of MYI in the last 3 years of our time series, and as such, are the areas most primed for future expansion of ice algal habitat. However, bottom ice melt date, not snow depth or ice thickness, was the primary predictor of habitat variability in the Nordic region, implying that a greater proportion of FYI would not greatly benefit ice algae there. This finding leaves the Central Arctic as the final frontier for increasing ice algal habitat by the mechanisms highlighted in this study: increased light transmission through younger, thinner ice with a thinner snow cover. Finally, we predict that increases in ice algal habitat will not continue indefinitely as the Arctic continues to melt. Once MYI disappears from the Arctic Ocean, the trend in ice algal habitat will likely reverse, and ice algal habitat will begin to decline. The most recent CMIP6 simulations predict that the Arctic Ocean will reach the turning point of ice-free summers around 2050 (**Figure 3C**; Notz and Community, 2020). After that, ice and snow may continue to thin somewhat due to warming temperatures, changing precipitation patterns, and later freeze-up, but to little effect, as most FYI already transmits enough light to support ice algal growth. The Barents Sea during 1985–2018 is perhaps an example of where the rest of the Arctic Ocean is headed: ice algal habitat declined because habitat loss due to decreased ice extent (both FYI and MYI) outweighed any gain due to increased light transmission through thinner snow. Overall, decreases in total sea ice extent and the length of the sea ice season are likely to become the most pressing factors, with the future of ice algae dependent on the persistence of FYI in the Arctic Ocean.

Data accessibility statement
The data produced for this study are available at https://doi.org/10.25740/hn961zj6005. The citations for data used as inputs (e.g., ice age, snow depth, atmospheric reanalyses) are included directly in the text.

Supplemental files
The supplemental files for this article can be found as follows:
Figure S1. Table S1. PDF

Competing interests
The authors have no competing interests to declare. Kevin Arrigo is an associate editor at Elementa and was not involved in the review process of this article.

Author contributions
Contributed to conception and design: KRA, SML.
Contributed to acquisition of data: SML, GLvD.
Contributed to analysis and interpretation of data: SML, KRA, CMP, GLvD.
Drafted the article: SML.
Revised the article and approved the submitted version for publication: All authors.

References
Abraham, C, **Steiner, N**, **Monahan, A**, **Michel, C**. 2015. Effects of subgrid-scale snow thickness variability on radiative transfer in sea ice. *Journal of Geophysical Research: Oceans* **120**(8): 5597–5614. DOI: http://dx.doi.org/10.1002/2015JC010741.

Arctic Monitoring and Assessment Programme. 2019. *Arctic climate change update 2019: An update to key findings of snow, water, ice, and permafrost in the Arctic (SWIPA) 2017.* Available at http://www.amap.no/documents/doc/amap-climate-change-update-2019/1761.

Ambrose, WG, **von Quillfeldt, C**, **Clough, LM**, **Tilney, PVR**, **Tucker, T**. 2005. The sub-ice algal community in the Chukchi Sea: Large- and small-scale patterns of abundance based on images from a remotely operated vehicle. *Polar Biology* **28**(10): 784–795. DOI: http://dx.doi.org/10.1007/s00300-005-0002-8.

Arrigo, KR. 2017. Sea ice as a habitat for primary producers, in Thomas, DN ed., *Sea ice.* 3rd ed. Chichester, UK: John Wiley & Sons, Ltd: 352–369.

Arrigo, KR, **Sullivan, CW**, **Kremer, JN**. 1991. A bio-optical model of Antarctic sea ice. *Journal of Geophysical Research* **96**(C6): 10581. DOI: http://dx.doi.org/10.1029/91JC00455.

Arrigo, KR, **Worthen, DL**, **Dixon, PL**, **Lizotte, MP**. 1998. Primary productivity of near surface communities within Antarctic pack ice, in Lizotte, P, Arrigo, R eds., *Antarctic research series* (vol. **73**). Washington, DC: American Geophysical Union: 23–43. DOI:

https://agupubs.onlinelibrary.wiley.com/doi/10.1029/AR073p0023.

Assmy, P, Fernández-Méndez, M, Duarte, P, Meyer, A, Randelhoff, A, Mundy, CJ, Olsen, LM, Kauko, HM, Bailey, A, Chierici, M, Cohen, L, Doulgeris, AP, Ehn, JK, Fransson, A, Gerland, S, Hop, H, Hudson, SR, Hughes, N, Itkin, P, Johnsen, G, King, JA, Koch, BP, Koenig, Z, Kwasniewski, S, Laney, SR, Nicolaus, M, Pavlov, AK, Polashenski, CM, Provost, C, Rösel, A, Sandbu, M, Spreen, G, Smedsrud, LH, Sundfjord, A, Taskjelle, T, Tatarek, A, Wiktor, J, Wagner, PM, Wold, A, Steen, H, Granskog, MA. 2017. Leads in Arctic pack ice enable early phytoplankton blooms below snow-covered sea ice. *Scientific Reports* **7**(1): 40850. DOI: http://dx.doi.org/10.1038/srep40850.

Barrett, AP, Stroeve, JC, Serreze, MC. 2020. Arctic Ocean precipitation from atmospheric reanalyses and comparisons with North Pole drifting station records. *Journal of Geophysical Research: Oceans* **125**(1). DOI: http://dx.doi.org/10.1029/2019JC015415.

Bélanger, S, Babin, M, Tremblay, JÉ. 2013. Increasing cloudiness in Arctic damps the increase in phytoplankton primary production due to sea ice receding. *Biogeosciences* **10**(6): 4087–4101. DOI: http://dx.doi.org/10.5194/bg-10-4087-2013.

Bergmann, MA, Welch, HE, Butler-Walker, JE, Siferd, TD. 1991. Ice algal photosynthesis at resolute and saqvaqjuac in the Canadian Arctic. *Journal of Marine Systems* **2**(1–2): 43–52. DOI: http://dx.doi.org/10.1016/0924-7963(91)90012-J.

Blanchard-Wrigglesworth, E, Farrell, SL, Newman, T, Bitz, CM. 2015. Snow cover on Arctic sea ice in observations and an earth system model. *Geophysical Research Letters* **42**(23): 10342–10348. DOI: http://dx.doi.org/10.1002/2015GL066049.

Bluhm, BA, Swadling, KM, Gradinger, R. 2017. Sea ice as a habitat for macrograzers, in Thomas, DN ed., *Sea ice*. 3rd ed. Chichester, UK: John Wiley & Sons, Ltd: 394–414. DOI: http://dx.doi.org/10.1002/9781118778371.ch16.

Boetius, A, Albrecht, S, Bakker, K, Bienhold, C, Felden, J, Fernandez-Mendez, M, Hendricks, S, Katlein, C, Lalande, C, Krumpen, T, Nicolaus, M, Peeken, I, Rabe, B, Rogacheva, A, Rybakova, E, Somavilla, R, Wenzhofer, F, RV Polarstern ARK27-3-Shipboard Science Party. 2013. Export of algal biomass from the melting Arctic sea ice. *Science* **339**(6126): 1430–1432. DOI: http://dx.doi.org/10.1126/science.1231346.

Campbell, K, Mundy, CJ, Barber, DG, Gosselin, M. 2015. Characterizing the sea ice algae chlorophyll *a*-snow depth relationship over Arctic spring melt using transmitted irradiance. *Journal of Marine Systems* **147**: 76–84. DOI: http://dx.doi.org/10.1016/j.jmarsys.2014.01.008.

Carmack, E, Barber, D, Christensen, J, Macdonald, R, Rudels, B, Sakshaug, E. 2006. Climate variability and physical forcing of the food webs and the carbon budget on panarctic shelves. *Progress in Oceanography* **71**(2–4): 145–181. DOI: http://dx.doi.org/10.1016/j.pocean.2006.10.005.

Caron, DA, Gast, RJ, Garneau, MÈ. 2017. Sea ice as a habitat for micrograzers, in Thomas, DN ed., *Sea ice*. 3rd ed. Chichester, UK: John Wiley & Sons, Ltd: 370–393. DOI: http://dx.doi.org/10.1002/9781118778371.ch15.

Carvalho, K, Wang, S. 2020. Sea surface temperature variability in the Arctic Ocean and its marginal seas in a changing climate: Patterns and mechanisms. *Global and Planetary Change* **193**: 103265. DOI: http://dx.doi.org/10.1016/j.gloplacha.2020.103265.

Codispoti, L, Kelly, V, Thessen, A, Matrai, P, Suttles, S, Hill, V, Steele, M, Light, B. 2013. Synthesis of primary production in the Arctic Ocean: III. Nitrate and phosphate based estimates of net community production. *Progress in Oceanography* **110**: 126–150. DOI: http://dx.doi.org/10.1016/j.pocean.2012.11.006.

Conover, RJ. 1988. Comparative life histories in the genera *Calanus and Neocalanus* in high latitudes of the northern hemisphere. *Hydrobiologia* **167−168**(1): 127–142. DOI: http://dx.doi.org/10.1007/BF00026299.

Cota, GF. 1985. Photoadaptation of high Arctic ice algae. *Nature* **315**(6016): 219–222. DOI: http://dx.doi.org/10.1038/315219a0.

Deal, C, Jin, M, Elliott, S, Hunke, E, Maltrud, M, Jeffery, N. 2011. Large-scale modeling of primary production and ice algal biomass within Arctic sea ice in 1992. *Journal of Geophysical Research: Oceans* **116**(7): 1–14. DOI: http://dx.doi.org/10.1029/2010JC006409.

Dobson, FW, Smith, SD. 1988. Bulk models of solar radiation at sea. *Quarterly Journal of the Royal Meteorological Society* **114**(479): 165–182. DOI: http://dx.doi.org/10.1002/qj.49711447909.

Dupont, F. 2012. Impact of sea-ice biology on overall primary production in a biophysical model of the pan-Arctic Ocean. *Journal of Geophysical Research: Oceans* **117**(8): 1–18. DOI: http://dx.doi.org/10.1029/2011JC006983.

Durbin, EG, Casas, MC. 2014. Early reproduction by *Calanus glacialis* in the Northern Bering Sea: The role of ice algae as revealed by molecular analysis. *Journal of Plankton Research* **36**(2): 523–541. DOI: http://dx.doi.org/10.1093/plankt/fbt121.

Falk-Petersen, S, Mayzaud, P, Kattner, G, Sargent, JR. 2009. Lipids and life strategy of Arctic *Calanus*. *Marine Biology Research* **5**(1): 18–39. DOI: http://dx.doi.org/10.1080/17451000802512267.

Fortier, M, Fortier, L, Michel, C, Legendre, L. 2002. Climatic and biological forcing of the vertical flux of biogenic particles under seasonal Arctic sea ice. *Marine Ecology Progress Series* **225**: 1–16. DOI: http://dx.doi.org/10.3354/meps225001.

Fox, J, Weisberg, S. 2019. *An R companion to applied regression*. 3rd ed. Thousand Oaks, CA: Sage.

Francis, JA, **Vavrus, SJ**, **Cohen, J**. 2017. Amplified Arctic warming and mid-latitude weather: New perspectives on emerging connections. *WIREs Climate Change* **8**(5). DOI: http://dx.doi.org/10.1002/wcc.474.

Garrison, DL, **Ackley, SF**, **Buck, KR**. 1983. A physical mechanism for establishing algal populations in frazil ice. *Nature* **306**(5941): 363–365. DOI: http://dx.doi.org/10.1038/306363a0.

Gosselin, M, **Legendre, L**, **Demers, S**, **Ingram, RG**. 1985. Responses of sea-ice microalgae to climatic and fortnightly tidal energy inputs (Manitounuk Sound, Hudson Bay). *Canadian Journal of Fisheries and Aquatic Sciences* **42**(5): 999–1006. DOI: http://dx.doi.org/10.1139/f85-125.

Gosselin, M, **Legendre, L**, **Therriault, JC**, **Demers, S**, **Rochet, M**. 1986. Physical control of the horizontal patchiness of sea-ice microalgae. *Marine Ecology Progress Series* **29**: 289–298. DOI: http://dx.doi.org/10.3354/meps029289.

Gosselin, M, **Levasseur, M**, **Wheeler, PA**. 1997. New measurements of phytoplankton and ice algal production in the Arctic Ocean. *Deep Sea Research Part II: Topical Studies in Oceanography* **44**(8): 1623–1644. DOI: http://dx.doi.org/10.1016/S0967-0645(97)00054-4.

Gradinger, R. 1999. Vertical fine structure of the biomass and composition of algal communities in Arctic pack ice. *Marine Biology* **133**: 745–754. DOI: http://dx.doi.org/10.1007/s002270050516.

Gradinger, R, **Ikävalko, J**. 1998. Organism incorporation into newly forming Arctic sea ice in the Greenland Sea. *Journal of Plankton Research* **20**(5): 871–886. DOI: http://dx.doi.org/10.1093/plankt/20.5.871.

Gregg, WW, **Carder, KL**. 1990. A simple spectral solar irradiance model for cloudless maritime atmospheres. *Limnology and Oceanography* **35**(8): 1657–1675. DOI: http://dx.doi.org/10.4319/lo.1990.35.8.1657.

Grömping, U. 2006. Relative importance for linear regression in R: The package Relaimpo. *Journal of Statistical Software* **17**(1): 1–27. DOI: http://dx.doi.org/10.18637/jss.v017.i01.

Grossi, SMG, **Kottmeier, ST**, **Moe, RL**, **Taylor, GT**, **Sullivan, CW**. 1987. Sea ice microbial communities. VI. Growth and primary production in bottom ice under graded snow cover. *Marine Ecology Progress Series* **35**: 153–164. DOI: http://dx.doi.org/10.3354/meps035153.

Hancke, K, **Lund-Hansen, LC**, **Lamare, ML**, **Højlund Pedersen, S**, **King, MD**, **Andersen, P**, **Sorrell, BK**. 2018. Extreme low light requirement for algae growth underneath sea ice: A case study from station nord, NE Greenland. *Journal of Geophysical Research: Oceans* **123**(2): 985–1000. DOI: http://dx.doi.org/10.1002/2017JC013263.

Horner, R, **Schrader, G**. 1982. Relative contributions of ice algae, phytoplankton, and benthic microalgae to primary production in nearshore regions of the Beaufort Sea. *ARCTIC* **35**(4): 485–503. DOI: http://dx.doi.org/10.14430/arctic2356.

Hussain, M, **Mahmud, I**. 2019. pyMannKendall: A python package for non parametric Mann Kendall family of trend tests. *Journal of Open Source Software* **4**(39): 1556. DOI: http://dx.doi.org/10.21105/joss.01556.

James, G, **Witten, D**, **Hastie, T**, **Tibshirani, R**. 2013. *An introduction to statistical learning*. New York, NY: Springer New York. (Springer texts in statistics; vol. 103). DOI: http://dx.doi.org/10.1007/978-1-4614-7138-7.

Ji, R, **Jin, M**, **Varpe, Ø**. 2013. Sea ice phenology and timing of primary production pulses in the Arctic Ocean. *Global Change Biology* **19**(3): 734–741. DOI: http://dx.doi.org/10.1111/gcb.12074.

Jin, M, **Deal, C**, **Lee, SH**, **Elliott, S**, **Hunke, E**, **Maltrud, M**, **Jeffery, N**. 2012. Investigation of Arctic sea ice and ocean primary production for the period 1992-2007 using a 3-D global ice-ocean ecosystem model. *Deep Sea Research Part II: Topical Studies in Oceanography* **81−84**: 28–35. DOI: http://dx.doi.org/10.1016/j.dsr2.2011.06.003.

Juhl, AR, **Krembs, C**. 2010. Effects of snow removal and algal photoacclimation on growth and export of ice algae. *Polar Biology* **33**(8): 1057–1065. DOI: http://dx.doi.org/10.1007/s00300-010-0784-1.

Kalnay, E, **Kanamitsu, M**, **Kistler, R**, **Collins, W**, **Deaven, D**, **Gandin, L**, **Iredell, M**, **Saha, S**, **White, G**, **Woollen, J**, **Zhu, Y**, **Chelliah, M**, **Ebisuzaki, W**, **Higgens, W**, **Janowiak, J**, **Mo, K**, **Ropelewski, C**, **Wang, J**, **Leetmaa, A**, **Reynolds, R**, **Jenne, R**, **Joseph, D**. 1996. The NCEP/NCAR 40-year reanalysis project. *Bulletin of the American Meteorological Society* **77**: (437–470). DOI: http://dx.doi.org/10.1175/1520-0477(1996)077<0437:TNYRP>2.0.CO;2.

Katlein, C, **Arndt, S**, **Nicolaus, M**, **Perovich, DK**, **Jakuba, MV**, **Suman, S**, **Elliott, S**, **Whitcomb, LL**, **McFarland, CJ**, **Gerdes, R**, **Boetius, A**, **German, CR**. 2015. Influence of ice thickness and surface properties on light transmission through Arctic sea ice. *Journal of Geophysical Research: Oceans* **120**(9): 5932–5944. DOI: http://dx.doi.org/10.1002/2015JC010914.

Kauko, HM, **Olsen, LM**, **Duarte, P**, **Peeken, I**, **Granskog, MA**, **Johnsen, G**, **Fernández-Méndez, M**, **Pavlov, AK**, **Mundy, CJ**, **Assmy, P**. 2018. Algal colonization of young Arctic sea ice in spring. *Frontiers in Marine Science* **5**(JUN): 199. DOI: http://dx.doi.org/10.3389/fmars.2018.00199.

Kauko, HM, **Taskjelle, T**, **Assmy, P**, **Pavlov, AK**, **Mundy, CJ**, **Duarte, P**, **Fernández-Méndez, M**, **Olsen, LM**, **Hudson, SR**, **Johnsen, G**, **Elliott, A**, **Wang, F**, **Granskog, MA**. 2017. Windows in Arctic sea ice: Light transmission and ice algae in a refrozen lead. *Journal of Geophysical Research: Biogeosciences* **122**(6): 1486–1505. DOI: http://dx.doi.org/10.1002/2016JG003626.

Kendall, MG. 1975. *Rank correlation methods*. London, UK: Griffin.

Kohlbach, D, **Graeve, M**, **Lange, BA**, **David, C**, **Peeken, I**, **Flores, H**. 2016. The importance of ice algae-produced carbon in the Central Arctic Ocean ecosystem: Food web relationships revealed by lipid and stable isotope analyses. *Limnology and Oceanography* **61**(6): 2027–2044. DOI: http://dx.doi.org/10.1002/lno.10351.

Kwok, R. 2018. Arctic sea ice thickness, volume, and multiyear ice coverage: Losses and coupled variability (1958-2018). *Environmental Research Letters* **13**(10): 105005. DOI: http://dx.doi.org/10.1088/1748-9326/aae3ec.

Lalande, C, **Grebmeier, JM**, **Hopcroft, RR**, **Danielson, SL**. 2020. Annual cycle of export fluxes of biogenic matter near Hanna Shoal in the northeast Chukchi Sea. *Deep Sea Research Part II: Topical Studies in Oceanography* **177**: 104730. DOI: http://dx.doi.org/10.1016/j.dsr2.2020.104730.

Lange, BA, **Flores, H**, **Michel, C**, **Beckers, JF**, **Castellani, G**, **Hatam, I**, **Bublitz, A**, **Alec, J**, **Reppchen, A**, **Rudolph, SA**, **Haas, C**. 2017. Pan-Arctic sea ice-algal chl *a* biomass and suitable habitat are largely underestimated for multiyear ice. *Global Change Biology* **23**: 4581–4597. DOI: http://dx.doi.org/10.1111/gcb.13742.

Lange, BA, **Michel, C**, **Beckers, JF**, **Casey, JA**, **Flores, H**, **Hatam, I**, **Meisterhans, G**, **Niemi, A**, **Haas, C**. 2015. Comparing springtime ice-algal chlorophyll a and physical properties of multi-year and first-year sea ice from the Lincoln Sea. *PLoS One* **10**(4): e0122418. DOI: http://dx.doi.org/10.1371/journal.pone.0122418.

Lavoie, D, **Denman, K**, **Michel, C**. 2005. Modeling ice algal growth and decline in a seasonally ice-covered region of the Arctic (Resolute Passage, Canadian Archipelago). *Journal of Geophysical Research* **110**: 11009. DOI: http://dx.doi.org/10.1029/2005JC002922.

Legendre, L, **Ackley, SF**, **Dieckmann, G**, **Gulliksen, B**, **Horner, R**, **Hoshiai, T**, **Melnikov, I**, **Reeburgh, W**, **Spindler, M**, **Sullivan, C**. 1992. Ecology of sea ice biota: 2. Global significance. *Polar Biology* **12**(3–4): 429–444. DOI: http://dx.doi.org/10.1007/bf00243114.

Leu, E, **Mundy, CJ**, **Assmy, P**, **Campbell, K**, **Gabrielsen, TM**, **Gosselin, M**, **Juul-Pedersen, T**, **Gradinger, R**. 2015. Arctic spring awakening—Steering principles behind the phenology of vernal ice algal blooms. *Progress in Oceanography* **139**: 151–170. DOI: http://dx.doi.org/10.1016/j.pocean.2015.07.012.

Lewis, KM, **van Dijken, GL**, **Arrigo, KR**. 2020. Changes in phytoplankton concentration, not sea ice, now drive increased Arctic Ocean primary production. *Science*. DOI: http://dx.doi.org/10.1126/science.aay8380.

Lindeman, RH, **Merenda, PF**, **Gold, RZ**. 1980. *Introduction to bivariate and multivariate analysis*. Glenview, IL: Scott, Foresman.

Liston, GE, **Itkin, P**, **Stroeve, J**, **Tschudi, M**, **Stewart, JS**, **Pedersen, SH**, **Reinking, AK**, **Elder, K**. 2020. A lagrangian snow-evolution system for sea-ice applications (SnowModel-LG): Part I—Model description. *Journal of Geophysical Research: Oceans* **125**: e2019JC015913. DOI: http://dx.doi.org/10.1029/2019jc015913.

Mann, HB. 1945. Nonparametric tests against trend. *Econometrica* **13**(3): 245. DOI: http://dx.doi.org/10.2307/1907187.

Maslanik, JA, **Fowler, C**, **Stroeve, J**, **Drobot, S**, **Zwally, J**, **Yi, D**, **Emery, W**. 2007. A younger, thinner Arctic ice cover: Increased potential for rapid, extensive sea-ice loss. *Geophysical Research Letters* **34**(24): 2004–2008. DOI: http://dx.doi.org/10.1029/2007GL032043.

McConnell, B, **Gradinger, R**, **Iken, K**, **Bluhm, BA**. 2012. Growth rates of Arctic juvenile *Scolelepis squamata* (Polychaeta: Spionidae) isolated from Chukchi Sea fast ice. *Polar Biology* **35**(10): 1487–1494. DOI: http://dx.doi.org/10.1007/s00300-012-1187-2.

Meiners, KM, **Michel, C**. 2017. Dynamics of nutrients, dissolved organic matter and exopolymers in sea ice, in Thomas, DN ed., *Sea ice*. 3rd ed. Chichester, UK: John Wiley & Sons, Ltd: 415–432. DOI: http://dx.doi.org/10.1002/9781118778371.ch17.

Melnikov, IA, **Kolosova, EG**, **Welch, HE**, **Zhitina, LS**. 2002. Sea ice biological communities and nutrient dynamics in the Canada Basin of the Arctic Ocean. *Deep Sea Research Part I: Oceanographic Research Papers* **49**(9): 1623–1649. DOI: http://dx.doi.org/10.1016/S0967-0637(02)00042-0.

Mock, T, **Gradinger, R**. 1999. Determination of Arctic ice algal production with a new *in situ* incubation technique. *Marine Ecology Progress Series* **177**(Melnikov 1997): 15–26. DOI: http://dx.doi.org/10.3354/meps177015.

Mortenson, E, **Hayashida, H**, **Steiner, N**, **Monahan, A**, **Blais, M**, **Gale, MA**, **Galindo, V**, **Gosselin, M**, **Hu, X**, **Lavoie, D**, **Mundy, CJ**. 2017. A model-based analysis of physical and biological controls on ice algal and pelagic primary production in Resolute Passage. *Elementa: Science of the Anthropocene* **5**: 39. DOI: http://dx.doi.org/10.1525/elementa.229.

Mundy, C, **Barber, D**, **Michel, C**. 2005. Variability of snow and ice thermal, physical and optical properties pertinent to sea ice algae biomass during spring. *Journal of Marine Systems* **58**(3–4): 107–120. DOI: http://dx.doi.org/10.1016/j.jmarsys.2005.07.003.

Notz, D, **Community, S**. 2020. Arctic sea ice in CMIP6. *Geophysical Research Letters* **47**(10): e2019GL086749. DOI: http://dx.doi.org/10.1029/2019GL086749.

Notz, D, **Worster, MG**. 2009. Desalination processes of sea ice revisited. *Journal of Geophysical Research* **114**(C5): C05006. DOI: http://dx.doi.org/10.1029/2008JC004885.

Nozais, C, **Gosselin, M**, **Michel, C**, **Tita, G**. 2001. Abundance, biomass, composition and grazing impact of the sea-ice meiofauna in the North Water, northern Baffin Bay. *Marine Ecology Progress Series* **217**: 235–250. DOI: http://dx.doi.org/10.3354/meps217235.

Olsen, LM, Laney, SR, Duarte, P, Kauko, HM, Fernández-Méndez, M, Mundy, CJ, Rösel, A, Meyer, A, Itkin, P, Cohen, L, Peeken, I, Tatarek, A, Różańska-Pluta, M, Wiktor, J, Taskjelle, T, Pavlov, AK, Hudson, SR, Granskog, MA, Hop, H, Assmy, P. 2017. The seeding of ice algal blooms in Arctic pack ice: The multiyear ice seed repository hypothesis. *Journal of Geophysical Research: Biogeosciences* **122**(7): 1529–1548. DOI: http://dx.doi.org/10.1002/2016JG003668.

Onarheim, IH, Eldevik, T, Smedsrud, LH, Stroeve, JC. 2018. Seasonal and regional manifestation of Arctic sea ice loss. *Journal of Climate* **31**(12): 4917–4932. DOI: http://dx.doi.org/10.1175/JCLI-D-17-0427.1.

Overland, JE, Wang, M, Ballinger, TJ. 2018. Recent increased warming of the Alaskan marine Arctic due to midlatitude linkages. *Advances in Atmospheric Sciences* **35**(1): 75–84. DOI: http://dx.doi.org/10.1007/s00376-017-7026-1.

Oziel, L, Massicotte, P, Randelhoff, A, Ferland, J, Vladoiu, A, Lacour, L, Galindo, V, Lambert-Girard, S, Dumont, D, Cuypers, Y, Bouruet-Aubertot, P, Mundy, CJ, Ehn, J, Bécu, G, Marec, C, Forget, MH, Garcia, N, Coupel, P, Raimbault, P, Houssais, MN, Babin, M. 2019. Environmental factors influencing the seasonal dynamics of spring algal blooms in and beneath sea ice in Western Baffin Bay. *Elementa: Science of the Anthropocene* **7**(1): 34. DOI: http://dx.doi.org/10.1525/elementa.372.

Parkinson, CL. 2014. Spatially mapped reductions in the length of the Arctic sea ice season. *Geophysical Research Letters* **41**(12): 4316–4322. DOI: http://dx.doi.org/10.1002/2014GL060434.

Payne, CM, Bianucci, L, Dijken, GL, Arrigo, KR. 2021. Changes in under-ice primary production in the Chukchi Sea from 1988 to 2018. *Journal of Geophysical Research: Oceans* **126**(9): e2021JC017483. DOI: http://dx.doi.org/10.1029/2021JC017483.

Perovich, DK. 2002. Seasonal evolution of the albedo of multiyear Arctic sea ice. *Journal of Geophysical Research* **107**(C10): 8044. DOI: http://dx.doi.org/10.1029/2000JC000438.

Perovich, DK. 2011. The changing Arctic sea ice cover. *Oceanography* **24**(3): 162–173. DOI: http://dx.doi.org/10.5670/oceanog.2011.68.

Perovich, DK, Maykut, GA, Grenfell, TC. 1986. Optical properties of ice and snow in the polar oceans. I: Observations. Proceedings of SPIE 0637, Ocean Optics VIII (7 August 1986). DOI: http://dx.doi.org/10.1117/12.964238.

Post, E. 2017. Implications of earlier sea ice melt for phenological cascades in Arctic marine food webs. *Food Webs* **13**: 60–66. DOI: http://dx.doi.org/10.1016/j.fooweb.2016.11.002.

Randelhoff, A, Holding, J, Janout, M, Sejr, MK, Babin, M, Tremblay, JÉ, Alkire, MB, Oliver, H. 2020. Pan-Arctic ocean primary production constrained by turbulent nitrate fluxes. *Frontiers in Marine Science* **7**(March): 1–15. DOI: http://dx.doi.org/10.3389/fmars.2020.00150.

Renaud, PE, Riedel, A, Michel, C, Morata, N, Gosselin, M, Juul-Pedersen, T, Chiuchiolo, A. 2007. Seasonal variation in benthic community oxygen demand: A response to an ice algal bloom in the Beaufort Sea, Canadian Arctic? *Journal of Marine Systems* **67**(1–2): 1–12. DOI: http://dx.doi.org/10.1016/j.jmarsys.2006.07.006.

Różańska, M, Poulin, M, Gosselin, M. 2008. Protist entrapment in newly formed sea ice in the coastal Arctic Ocean. *Journal of Marine Systems* **74**(3–4): 887–901. DOI: http://dx.doi.org/10.1016/j.jmarsys.2007.11.009.

Runge, JA, Ingram, RG. 1988. Underice grazing by planktonic, calanoid copepods in relation to a bloom of ice microalgae in southeastern Hudson Bay. *Limnology and Oceanography* **33**(2): 280–286. DOI: http://dx.doi.org/10.4319/lo.1988.33.2.0280.

Rysgaard, S, Kühl, M, Glud, R, Würgler Hansen, J. 2001. Biomass, production and horizontal patchiness of sea ice algae in a high-Arctic fjord (Young Sound, NE Greenland). *Marine Ecology Progress Series* **223**: 15–26. DOI: http://dx.doi.org/10.3354/meps223015.

Selz, V, Laney, S, Arnsten, AE, Lewis, KM, Lowry, KE, Joy-Warren, HL, Mills, MM, van Dijken, GL, Arrigo, KR. 2018. Ice algal communities in the Chukchi and Beaufort Seas in spring and early summer: Composition, distribution, and coupling with phytoplankton assemblages. *Limnology and Oceanography* **63**(3): 1109–1133. DOI: http://dx.doi.org/10.1002/lno.10757.

Sen, PK. 1968. Estimates of the regression coefficient based on Kendall's tau. *Journal of the American Statistical Association* **63**(324): 1379–1389. DOI: http://dx.doi.org/10.1080/01621459.1968.10480934.

Søreide, JE, Leu, E, Berge, J, Graeve, M, Falk-Petersen, S. 2010. Timing of blooms, algal food quality and *Calanus glacialis* reproduction and growth in a changing Arctic. *Global Change Biology* **16**(11): 3154–3163. DOI: http://dx.doi.org/10.1111/j.1365-2486.2010.02175.x.

Sorrell, BK, Hawes, I, Stratmann, T, Lund-Hansen, LC. 2021. Photobiological effects on ice algae of a rapid whole-fjord loss of snow cover during spring growth in Kangerlussuaq, a west Greenland fjord. *Journal of Marine Science and Engineering* **9**(8): 814. DOI: http://dx.doi.org/10.3390/jmse9080814.

Stroeve, J, Liston, GE, Buzzard, S, Zhou, L, Mallett, R, Barrett, A, Tschudi, M, Tsamados, M, Itkin, P, Stewart, JS. 2020. A lagrangian snow evolution system for sea ice applications (SnowModel-LG): Part II—Analyses. *Journal of Geophysical Research: Oceans* **125**(10): e2019JC015900. DOI: http://dx.doi.org/10.1029/2019JC015900.

Stroeve, J, Notz, D. 2018. Changing state of Arctic sea ice across all seasons. *Environmental Research Letters* **13**(10): 103001. DOI: http://dx.doi.org/10.1088/1748-9326/aade56.

Stroeve, J, Vancoppenolle, M, Veyssiere, G, Lebrun, M, Castellani, G, Babin, M, Karcher, M, Landy, J, Liston, GE, Wilkinson, J. 2021. A multi-sensor and modeling approach for mapping light under sea ice during the ice-growth season. *Frontiers in Marine Science* **7**: 592337. DOI: http://dx.doi.org/10.3389/fmars.2020.592337.

Subba Rao, DV, Platt, T. 1984. Primary production of Arctic waters. *Polar Biology* **3**(4): 191–201. DOI: http://dx.doi.org/10.1007/BF00292623.

Suzuki, Y, Kudoh, S, Takahashi, M. 1997. Photosynthetic and respiratory characteristics of an Arctic ice algal community living in low light and low temperature conditions. *Journal of Marine Systems* **11**(1–2): 111–121. DOI: http://dx.doi.org/10.1016/S0924-7963(96)00032-2.

Syvertsen, EE. 1991. Ice algae in the Barents Sea: Types of assemblages, origin, fate and role in the ice-edge phytoplankton bloom. *Polar Research* **10**(1): 277–288. DOI: http://dx.doi.org/10.3402/polar.v10i1.6746.

Szymanski, A, Gradinger, R. 2016. The diversity, abundance and fate of ice algae and phytoplankton in the Bering Sea. *Polar Biology* **39**(2): 309–325. DOI: http://dx.doi.org/10.1007/s00300-015-1783-z.

Tedesco, L, Vichi, M. 2014. Sea ice biogeochemistry: A guide for modellers. *PLoS One* **9**(2). DOI: http://dx.doi.org/10.1371/journal.pone.0089217.

Tedesco, L, Vichi, M, Scoccimarro, E. 2019. Sea-ice algal phenology in a warmer Arctic. *Science Advances* **5**(5): eaav4830. DOI: http://dx.doi.org/10.1126/sciadv.aav4830.

Tedesco, L, Vichi, M, Thomas, DN. 2012. Process studies on the ecological coupling between sea ice algae and phytoplankton. *Ecological Modelling* **226**: 120–138. DOI: http://dx.doi.org/10.1016/j.ecolmodel.2011.11.011.

Tremblay, JÉ, Anderson, LG, Matrai, P, Coupel, P, Bélanger, S, Michel, C, Reigstad, M. 2015. Global and regional drivers of nutrient supply, primary production and CO_2 drawdown in the changing Arctic Ocean. *Progress in Oceanography* **139**: 171–196. DOI: http://dx.doi.org/10.1016/j.pocean.2015.08.009.

Tschudi, MA, Meier, WN, Stewart, JS. 2020. An enhancement to sea ice motion and age products at the national snow and ice data center (NSIDC). *Cryosphere* **14**(5): 1519–1536. DOI: http://dx.doi.org/10.5194/tc-14-1519-2020.

Tschudi, MA, Meier, WN, Stewart, JS, Fowler, C, Maslanik, JA. 2019. EASE-Grid Sea Ice Age, Version 4. DOI: http://dx.doi.org/10.5067/UTAV7490FEPB.

Tschudi, MA, Stroeve, JC, Stewart, JS. 2016. Relating the age of Arctic sea ice to its thickness, as measured during NASA's ICESat and IceBridge Campaigns. *Remote Sensing* **8**(6). DOI: http://dx.doi.org/10.3390/rs8060457.

van Leeuwe, MA, Tedesco, L, Arrigo, KR, Assmy, P, Campbell, K, Meiners, KM, Rintala, JM, Selz, V, Thomas, DN, Stefels, J, Deming, JW. 2018. Microalgal community structure and primary production in Arctic and Antarctic sea ice: A synthesis. *Elementa: Science of the Anthropocene* **6**(1). DOI: http://dx.doi.org/10.1525/elementa.267.

Virtanen, P, Gommers, R, Oliphant, TE, Haberland, M, Reddy, T, Cournapeau, D, Burovski, E, Peterson, P, Weckesser, W, Bright, J, van der Walt, SJ, Brett, M, Wilson, J, Millman, KJ, Mayorov, N, Nelson, ARJ, Jones, E, Kern, R, Larson, E, Carey, CJ, Polat, İ, Feng, Y, Moore, EW, VanderPlas, J, Laxalde, D, Perktold, J, Cimrman, R, Henriksen, I, Quintero, EA, Harris, CR, Archibald, AM, Ribeiro, AH, Pedregosa, F, van Mulbregt, P, Vijaykumar, A, Bardelli, AP, Rothberg, A, Hilboll, A, Kloeckner, A, Scopatz, A, Lee, A, Rokem, A, Woods, CN, Fulton, C, Masson, C, Häggström, C, Fitzgerald, C, Nicholson, DA, Hagen, DR, Pasechnik, DV, Olivetti, E, Martin, E, Wieser, E, Silva, F, Lenders, F, Wilhelm, F, Young, G, Price, GA, Ingold, GL, Allen, GE, Lee, GR, Audren, H, Probst, I, Dietrich, JP, Silterra, J, Webber, JT, Slavič, J, Nothman, J, Buchner, J, Kulick, J, Schönberger, JL, de Miranda Cardoso, JV, Reimer, J, Harrington, J, Rodríguez, JLC, Nunez-Iglesias, J, Kuczynski, J, Tritz, K, Thoma, M, Newville, M, Kümmerer, M, Bolingbroke, M, Tartre, M, Pak, M, Smith, NJ, Nowaczyk, N, Shebanov, N, Pavlyk, O, Brodtkorb, PA, Lee, P, McGibbon, RT, Feldbauer, R, Lewis, S, Tygier, S, Sievert, S, Vigna, S, Peterson, S, More, S, Pudlik, T, Oshima, T, Pingel, TJ, Robitaille, TP, Spura, T, Jones, TR, Cera, T, Leslie, T, Zito, T, Krauss, T, Upadhyay, U, Halchenko, YO, Vázquez-Baeza, Y. 2020. SciPy 1.0: Fundamental algorithms for scientific computing in Python. *Nature Methods* **17**(3): 261–272. DOI: http://dx.doi.org/10.1038/s41592-019-0686-2.

Wakatsuchi, M, Ono, N. 1983. Measurements of salinity and volume of brine excluded from growing sea ice. *Journal of Geophysical Research* **88**(C5): 2943. DOI: http://dx.doi.org/10.1029/JC088iC05p02943.

Watanabe, E, Jin, M, Hayashida, H, Zhang, J, Steiner, N. 2019. Multi-model intercomparison of the Pan-Arctic ice-algal productivity on seasonal, interannual, and decadal timescales. *Journal of Geophysical Research: Oceans* **124**(12): 9053–9084. DOI: http://dx.doi.org/10.1029/2019JC015100.

Watanabe, E, Onodera, J, Harada, N, Aita, MN, Ishida, A, Kishi, MJ. 2015. Wind-driven interannual variability of sea ice algal production in the western Arctic Chukchi Borderland. *Biogeosciences* **12**(20): 6147–6168. DOI: http://dx.doi.org/10.5194/bg-12-6147-2015.

Webster, MA, Rigor, IG, Nghiem, SV, Kurtz, NT, Farrell, SL, Perovich, DK, Sturm, M. 2014. Interdecadal changes in snow depth on Arctic sea ice. *Journal of Geophysical Research: Oceans* **119**: 5395–5406. DOI: http://dx.doi.org/10.1002/2014JC009985.

Wei, J, Zhang, X, Wang, Z. 2019. Reexamination of Fram Strait sea ice export and its role in recently accelerated Arctic sea ice retreat. *Climate Dynamics*

53(3–4): 1823–1841. DOI: http://dx.doi.org/10.1007/s00382-019-04741-0.

Welch, HE, **Bergmann, MA**. 1989. Seasonal development of ice algae and its prediction from environmental factors near Resolute, N.W.T., Canada. *Canadian Journal of Fisheries and Aquatic Sciences* **46**(10): 1793–1804. DOI: http://dx.doi.org/10.1139/f89-227.

Werner, I. 1997. Grazing of Arctic under-ice amphipods on sea-ice algae. *Marine Ecology Progress Series* **160**: 93–99. DOI: http://dx.doi.org/10.3354/meps160093.

Wiedmann, I, **Ershova, E**, **Bluhm, BA**, **Nöthig, EM**, **Gradinger, RR**, **Kosobokova, K**, **Boetius, A**. 2020. What feeds the benthos in the Arctic Basins? Assembling a carbon budget for the deep Arctic Ocean. *Frontiers in Marine Science* **7**: 224. DOI: http://dx.doi.org/10.3389/fmars.2020.00224.

You, Q, **Cai, Z**, **Pepin, N**, **Chen, D**, **Ahrens, B**, **Jiang, Z**, **Wu, F**, **Kang, S**, **Zhang, R**, **Wu, T**, **Wang, P**, **Li, M**, **Zuo, Z**, **Gao, Y**, **Zhai, P**, **Zhang, Y**. 2021. Warming amplification over the Arctic Pole and Third Pole: Trends, mechanisms and consequences. *Earth-Science Reviews* **217**: 103625. DOI: http://dx.doi.org/10.1016/j.earscirev.2021.103625.

Yue, S, **Wang, C**. 2004. The Mann-Kendall Test modified by effective sample size to detect trend in serially correlated hydrological series. *Water Resources Management* **18**(3): 201–218. DOI: http://dx.doi.org/10.1023/B: WARM.0000043140.61082.60.

Zeebe, RE, **Eicken, H**, **Robinson, DH**, **Wolf-Gladrow, D**, **Dieckmann, GS**. 1996. Modeling the heating and melting of sea ice through light absorption by microalgae. *Journal of Geophysical Research: Oceans* **101**(C1): 1163–1181. DOI: http://dx.doi.org/10.1029/95JC02687.

Zhang, J, **Ashjian, C**, **Campbell, R**, **Spitz, YH**, **Steele, M**, **Hill, V**. 2015. The influence of sea ice and snow cover and nutrient availability on the formation of massive under-ice phytoplankton blooms in the Chukchi Sea. *Deep Sea Research Part II: Topical Studies in Oceanography* **118**: 122–135. DOI: http://dx.doi.org/10.1016/j.dsr2.2015.02.008.

Zhang, J, **Spitz, YH**, **Steele, M**, **Ashjian, C**, **Campbell, R**, **Berline, L**, **Matrai, P**. 2010. Modeling the impact of declining sea ice on the Arctic marine planktonic ecosystem. *Journal of Geophysical Research: Oceans* **115**(10): 1–24. DOI: http://dx.doi.org/10.1029/2009JC005387.

ELEMENTA
Science of the Anthropocene

Elem Sci Anth is a peer-reviewed open access journal published by University of California Press.

OPEN ACCESS